

Supporting Information

Functional Design of Stimuli-Responsive Poly(phthalaldehyde)-based Adhesives:
Depolymerization Kinetics and Mechanical Strength Management through Plasticizer Addition

Patrick Damacet, Hana J. Yarbrough, Nicholas D. Blleloch, Hyuk-Jun Noh, and Katherine A.
Mirica*

Department of Chemistry, Burke Laboratory, Dartmouth College, Hanover, New Hampshire
03755, United States

Email: Katherine.A.Mirica@dartmouth.edu

Table of Contents

1. Synthetic procedures	2
1.1. Materials and methods	2
1.2. General procedure for the synthesis of poly(phthalaldehyde) with different endcaps	3
1.3. Purification procedure for PPA	4
1.4. Procedure for the synthesis of α-(isopropyl)-ω-(acetyl)-poly(phthalaldehyde) (IPA-PPA-Ac)	4
1.5. Procedure for the synthesis of α-(tert-butyldimethylsilyl)-ω-(tert-butyldimethylsilyl)-poly(phthalaldehyde) (TBS-PPA-TBS)	5
2. Spectroscopic characterization: $^1\text{H-NMR}$	5
3. Determination of the chemical, physical, and thermal properties of PPA	6
3.1 Gel permeation chromatography (GPC)	8
3.2 X-ray photoelectron spectroscopy (XPS)	9
3.3 Thermogravimetric analysis (TGA)	10
3.4 Differential scanning calorimetry (DSC)	11
4. Mechanical shearing strength of PPA	11
4.1 Solvent-assisted bonding of glass substrates	11
4.2 Shear testing of bonded assemblies for adhesive characterization	12
4.3 Melt bonding of substrates with poly(phthalaldehyde)/plasticizer material	19
4.4 Shear testing of PPA/DMP bonded assemblies for adhesive characterization	22

5. Acid triggered depolymerization of PPA	25
5.1. Acid-triggered depolymerization of IPA-PPA-Ac	25
5.2. Integrated rate laws	26
5.3. Residual plots significance	30
5.4 Cationic polymerization for the generation of cyclic poly(phthalaldehyde)	31
5.4.1 Synthesis of cyclic poly(phthalaldehyde) (cPPA).....	31
5.4.2 Spectroscopic characterization of cPPA.....	32
5.4.3 Chromatographic characterization of cPPA.....	33
5.4.4 Thermal characterization of cPPA.....	34
5.5. Acid-triggered decomposition of TBS-PPA-TBS and cPPA	35
5.6 Overestimation of the molecular weight of PPA via GPC measurements	36
5.7. Mechanism of the acid-catalyzed degradation of IPA-PPA-Ac	37
6. Fluoride-triggered depolymerization of PPA	38
6.1. Structural stability of PPA in DCM and DMSO solvents	38
6.2. Fluoride-triggered depolymerization of TBS-PPA-TBS	40
6.3. Integrated rate laws	42
6.4. Rapid kinetic screening of TBS-PPA-TBS decomposition	45
6.5. Effect of the nature of the tetra-<i>n</i>-butylammonium salt on TBS-PPA-TBS degradation rate	50
6.6. Mechanism of fluoride-catalyzed degradation of TBS-PPA-TBS	51
7. Solid-state depolymerization (SSD)	51
7.1 Preparation of TBS-PPA-TBS disks	51
7.2 Solid-state depolymerization (SSD) of TBS-PPA-TBS	51
7.3 Characterization of the SSD experiment product	52
8. Preparation of NYCO-bonded textiles on glass substrates	54
9. References	56

1. Synthetic procedures

1.1. Materials and methods

All glassware, magnetic bars, and stainless-steel syringe needles were oven-dried at 120 °C before performing reactions. Air-sensitive reactions were performed under argon atmosphere, where all reaction media, including syringes used for the transfer of liquids, were first purged with

argon. Starting materials were purchased from various suppliers and used directly without further purification. *o*-Phthalaldehyde (>99.5%, GC) was obtained from TCI. 1-*t*-Butyl-2,2,4,4,4-pentakis(dimethylamino)2I⁵,4I⁵-catenadi(phosphazene) (phosphazene base P₂-*t*-Bu 2M solution), *t*-butyldimethylsilanol (TBS-OH), *t*-butyldimethylsilylchloride (TBS-Cl), trifluoroacetic acid (TFA), 2-propanol (IPA, >99.5%), and acetyl chloride (98%, reagent grade) were acquired from Sigma-Aldrich. The solvents were purchased from Sigma Aldrich and used from the Sure/Seal™ bottles using a syringe and the cannulation technique unless otherwise noted. NMR spectra were recorded on a Bruker Ascend™, 600 MHz / 54 mm. Thermogravimetric analysis (TGA) measurements were carried out on a TGA 55 instrument with 10°C/min ramp rate and oxygen as a purge gas. Differential scanning calorimetry (DSC) measurements were performed on a DSC 250 instrument. X-ray photoelectron spectroscopy (XPS) experiments were carried out on Kratos Analytical AXIS Supra X-ray Photoelectron Spectrometer under ultrahigh vacuum (base pressure 10⁻⁷ Torr) equipped with a monochromatic Al (K α) X-ray source. Both survey and high-resolution spectra were obtained using a beam diameter of 200 μ m. Gel permeation chromatography (GPC) measurements were performed on “Waters GPC system” coupled with waters e2695 separations module and 2414 RI detector. Throughout all GPC measurements, tetrahydrofuran (THF, HPLC grade, >99.9%, inhibitor-free) was utilized as mobile phase.

1.2. General procedure for the synthesis of poly(phthalaldehyde) with different endcaps

Under argon atmosphere, 1,2-phthalaldehyde monomer (1 g, 7.4 mmol, 1 eq) was added to an oven-dried 50 mL round bottom flask (RBF) charged with a PTFE magnetic stirring bar. Anhydrous tetrahydrofuran (THF, 12 mL) was later added to the RBF using a disposable needle under positive pressure resulting in a final monomer concentration of 0.6 M. The resulting solution was degassed under argon for 15 minutes to ensure an oxygen-free atmosphere before the addition of the initiator. Subsequently, a specified amount of the alcohol initiator solution in THF (0.0074 mmol, 0.001 eq) was added, and the reaction mixture was allowed to stir for a few minutes, after which it was cooled down to -78 °C in an acetone/dry ice bath. This was followed by the addition of P₂-*t*-Bu base (0.1 mL, 0.37 mmol, 0.05 eq) in THF to the reaction mixture resulting in a vigorous reddish-orange solution. The reaction was allowed to stir for 2 hours at 600 rpm at a temperature of -78 °C after which the polymer was end-capped via the addition of pyridine (0.3 mL, 3.7 mmol, 0.5 eq) and a designated amount of the corresponding acyl chloride terminator (0.75 mmol, 0.1 eq) at -78 °C. Finally, the polymer solution was allowed to warm to RT while stirring for a few additional hours (4 to 12 hours) and was subsequently crashed with excess methanol (48 mL) resulting in a white precipitate. The resulting suspension was left to settle for a

few minutes after which it was collected over a Buchner funnel with a Whatman grade 5 filter paper. The resulting crude polymer was further washed with 50 mL of MeOH and dried under vacuum at room temperature for several hours before purification.

1.3. Purification procedure for PPA

The crude polymer was dissolved in pure THF to yield a 100 mg/mL solution and was subsequently transferred into a separatory funnel. The polymer was then crashed out of solution through its drop-wise addition into a methanol solution (given $V_{\text{MeOH}} = 10 \times V_{\text{THF}}$). The resulting white polymer precipitate was kept stirring in the solution for a few minutes and was thereafter collected using a Buchner funnel with a 55 mm Whatman grade 5 filter paper. Finally, the purified polymer was dried under vacuum (<1 torr) at RT for at least 24 h prior to characterization and determination of product yield.

1.4. Procedure for the synthesis of α -(isopropyl)- ω -(acetyl)-poly(phthalaldehyde) (IPA-PPA-Ac)

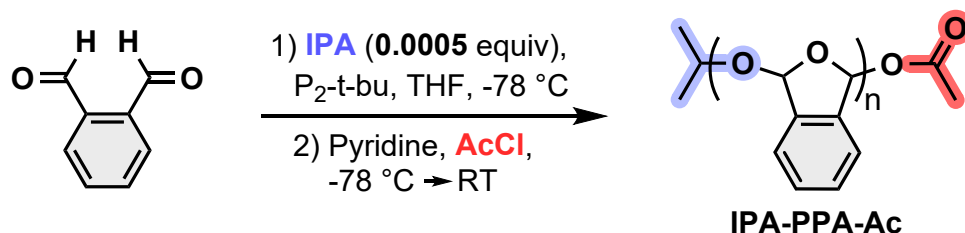


Figure S1. Synthesis procedure of IPA-PPA-Ac.

IPA-PPA-Ac was prepared on a 3 g monomer scale using 85 μL of a 1% dry IPA (V/V%) in THF (85 μL , 0.012 mmol, 0.0005 eq) as the initiator and first endcap, and acetyl chloride (0.16 mL, 2.24 mmol, 0.1 eq) as the terminator and second endcap to afford the purified white polymer material ($m = 2.3$ g).

1.5. Procedure for the synthesis of α -(tert-butyldimethylsilyl)- ω -(tert-butyldimethylsilyl)-poly(phthalaldehyde (TBS-PPA-TBS))

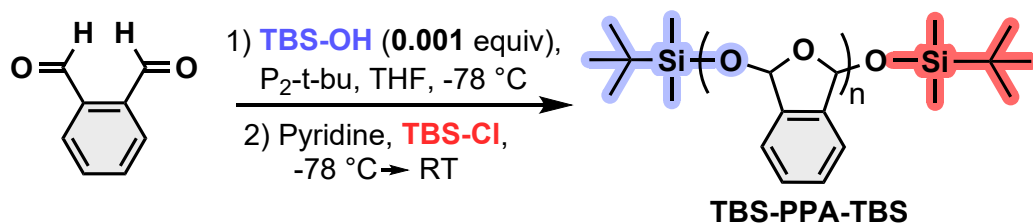


Figure S2. Synthesis procedure of TBS-PPA-TBS.

TBS-PPA-TBS was prepared on a 4 g monomer scale using TBS-OH in THF (23 μ L, 0.0311 mmol, 0.001 eq) as the initiator and first endcap, and TBS-Cl (0.47 mL, 3.11 mmol, 0.1 eq) as the terminator and second endcap to afford the purified white polymer material (m = 2.8 g).

2. Spectroscopic characterization: ¹H-NMR

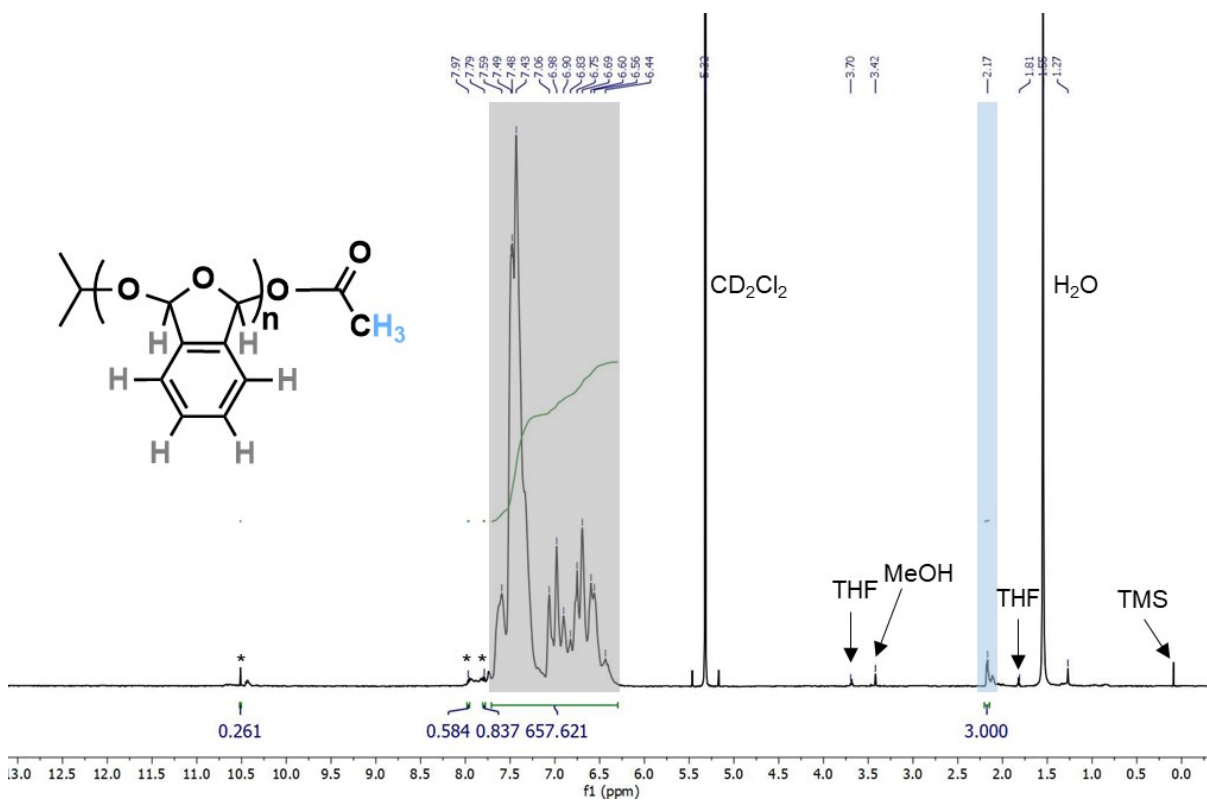


Figure S3. ¹H-NMR of IPA-PPA-Ac in CD₂Cl₂-d₂ at 600MHz. The asterisk "*" refers to the monomer peaks.

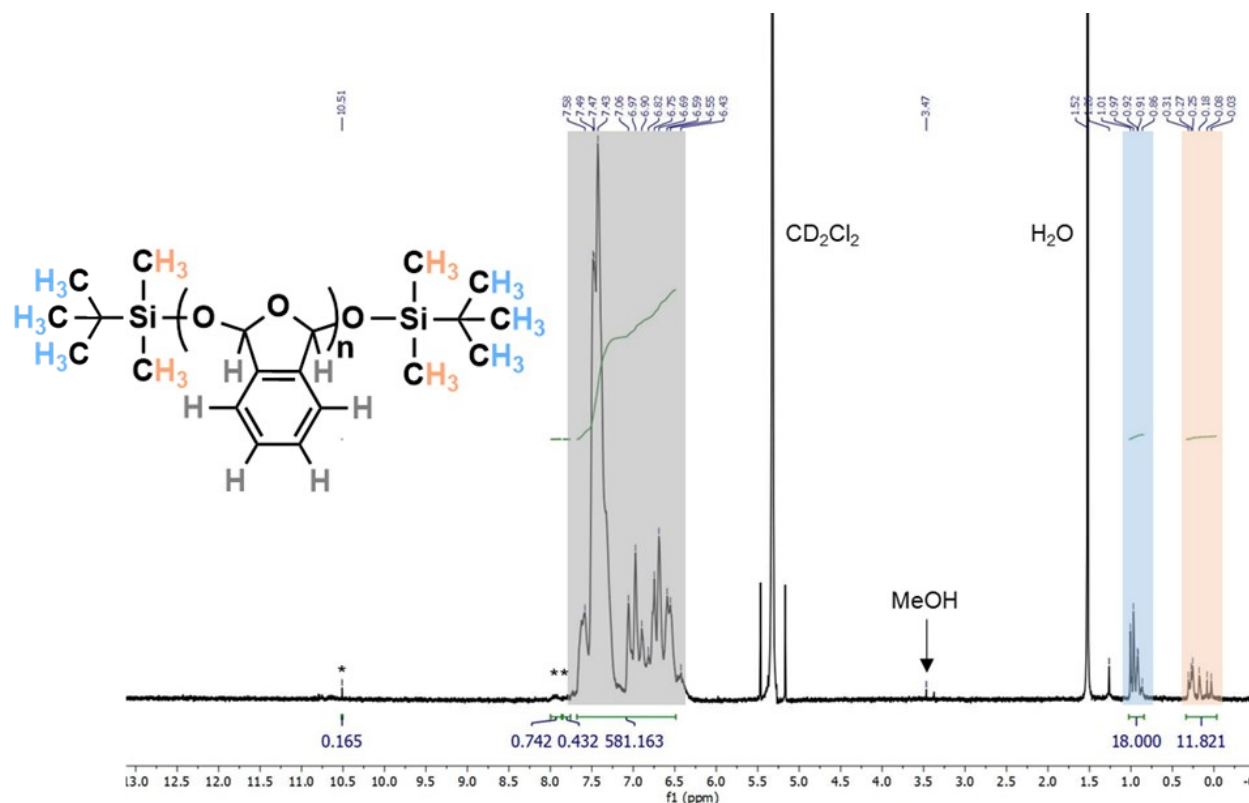


Figure S4. $^1\text{H-NMR}$ of TBS-PPA-TBS in $\text{CD}_2\text{Cl}_2\text{-d}_2$ at 600MHz. The asterisk “*” refers to monomer peaks.

3. Determination of the chemical, physical, and thermal properties of PPA

To determine the purity of PPA relative to the starting monomer, we first measured the integration curves of the monomer peaks at chemical shifts 7.8, 7.9, and 10.48 ppm, in addition to the polymer’s repeating unit peaks between 6.4 and 7.6 ppm. **Equation S1** was then utilized as follows:

$$\%Purity = \frac{I_{polymer}}{I_{monomer} + I_{polymer}} \times 100 \quad (\text{Equation S1})$$

Where $I_{polymer}$ represents the peak integration of PPA repeating units and $I_{monomer}$ represents the peak integrations of the monomer.

The degree of polymerization (D.P), known as number of repeating units, in addition to the number average molecular weights were determined via end-group analysis. For IPA-PPA-Ac,

the signal at 2.1 ppm originates from the acetyl protons and can be integrated and normalized to three as there are three protons at the end cap. The peaks of the repeating unit are then integrated and used in **Equation S2** below:

$$D.P = \frac{I_{\text{Polymer (normalized)}}}{n} \quad (\text{Equation S2})$$

Where $I_{\text{polymer (normalized)}}$ corresponds to the integration curves of the polymer repeating unit peaks after normalization and n represents the number of protons in the repeating unit, which in our case, is 6.

As for TBS-PPA-TBS, the signals at 0.05-0.4 and 0.8-1.05 ppm correspond to the two methyl groups and two *tert*-butyl groups, respectively.

Finally, the molecular weight is calculated by multiplying the degree of polymerization by the molar mass of the repeating monomeric unit using **Equation S3** as follows:

$$M_n = D.P \times M_{R.U} \quad (\text{Equation S3})$$

Where in our case $M_{R.U}$ (molar mass of the repeating unit) is 134.134 g/mol.

Characterization technique	Properties	IPA-PPA-Ac	TBS-PPA-TBS
Determined via ¹ H-NMR	Purity rel. to <i>o</i> -PA	99.8	99.8
	Number of repeating units	109	97
	Molecular Weight	14.7 KDa	12.9 KDa
Determined via GPC	Number Average Molecular Weight (M_n)	25.9 KDa	26.2 KDa
	Weight Average Molecular Weight (M_w)	39.8 KDa	39.1 KDa
	Polydispersity index	1.54	1.46
Determined via DSC	Melting point	169 °C	167 °C
Determined via TGA	Decomposition temperature	171 °C	172 °C

Table S1. Chemical and thermal properties of the prepared linear polymers as determined by ¹H-NMR, GPC, DSC, and TGA characterization techniques.

3.1 Gel permeation chromatography (GPC)

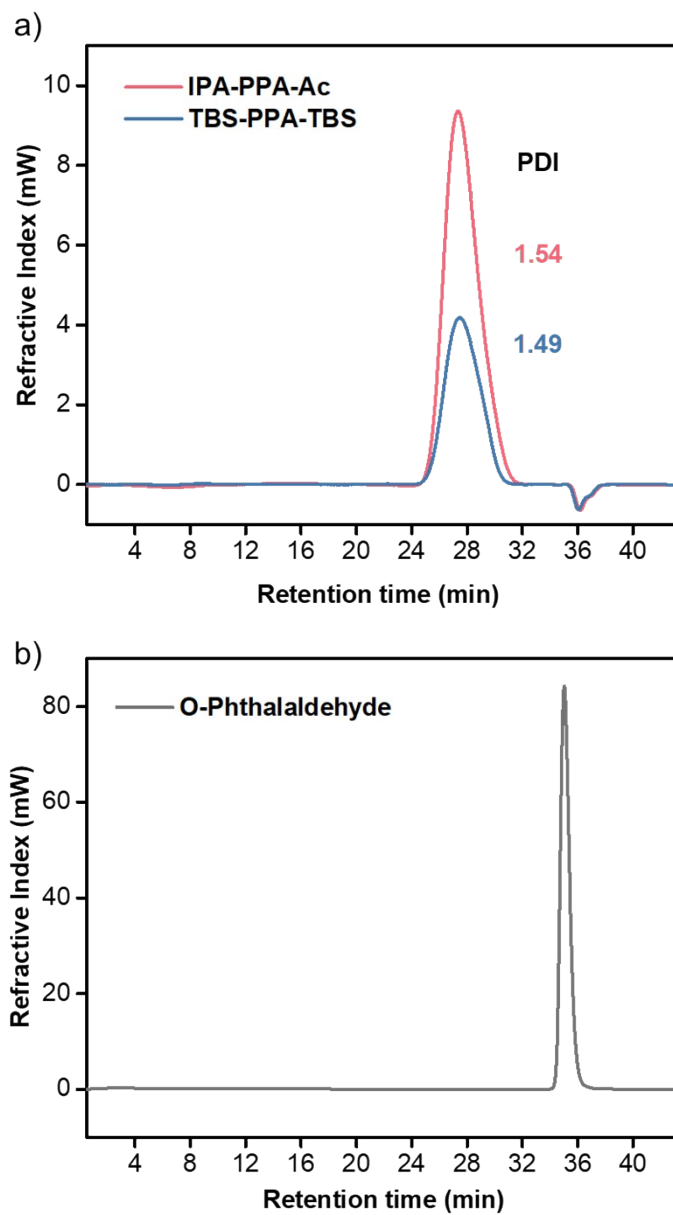


Figure S5. Representative GPC elution curves in THF for a) IPA-PPA-Ac and TBS-PPA-TBS, and b) pure *o*-phthalaldehyde precursor.

3.2. X-ray photoelectron spectroscopy (XPS)

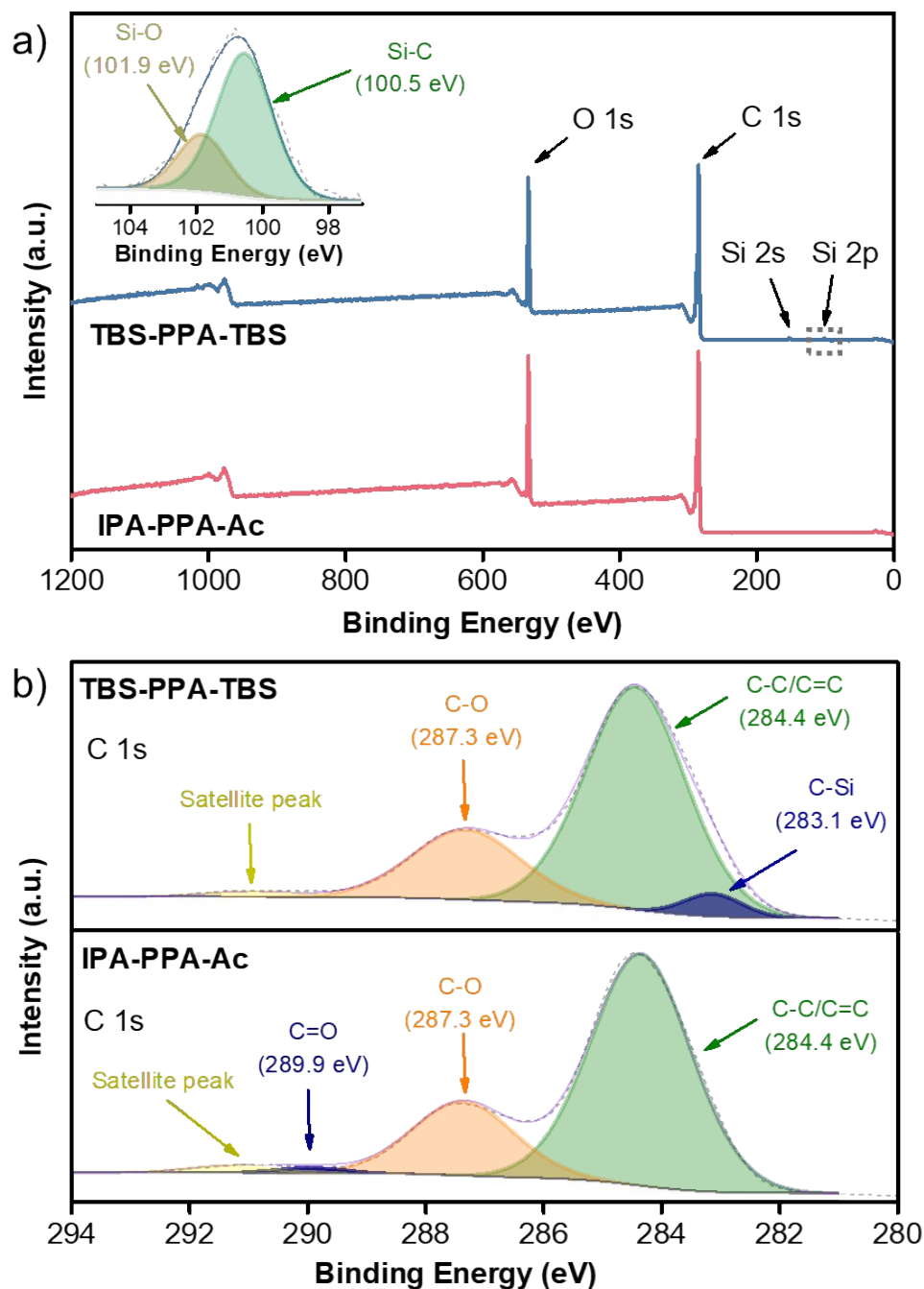


Figure S6. a) XPS survey of IPA-PPA-Ac and TBS-PPA-TBS. Inset: Deconvoluted Si 2p spectrum for TBS-PPA-TBS showing the presence of Si-C (100.5 eV) and Si-O (101.9 eV) bonds in the polymer. b) High resolution XPS spectra of the carbon (C 1s) region of both PPA polymers and their deconvolutions.

3.3. Thermogravimetric analysis (TGA)

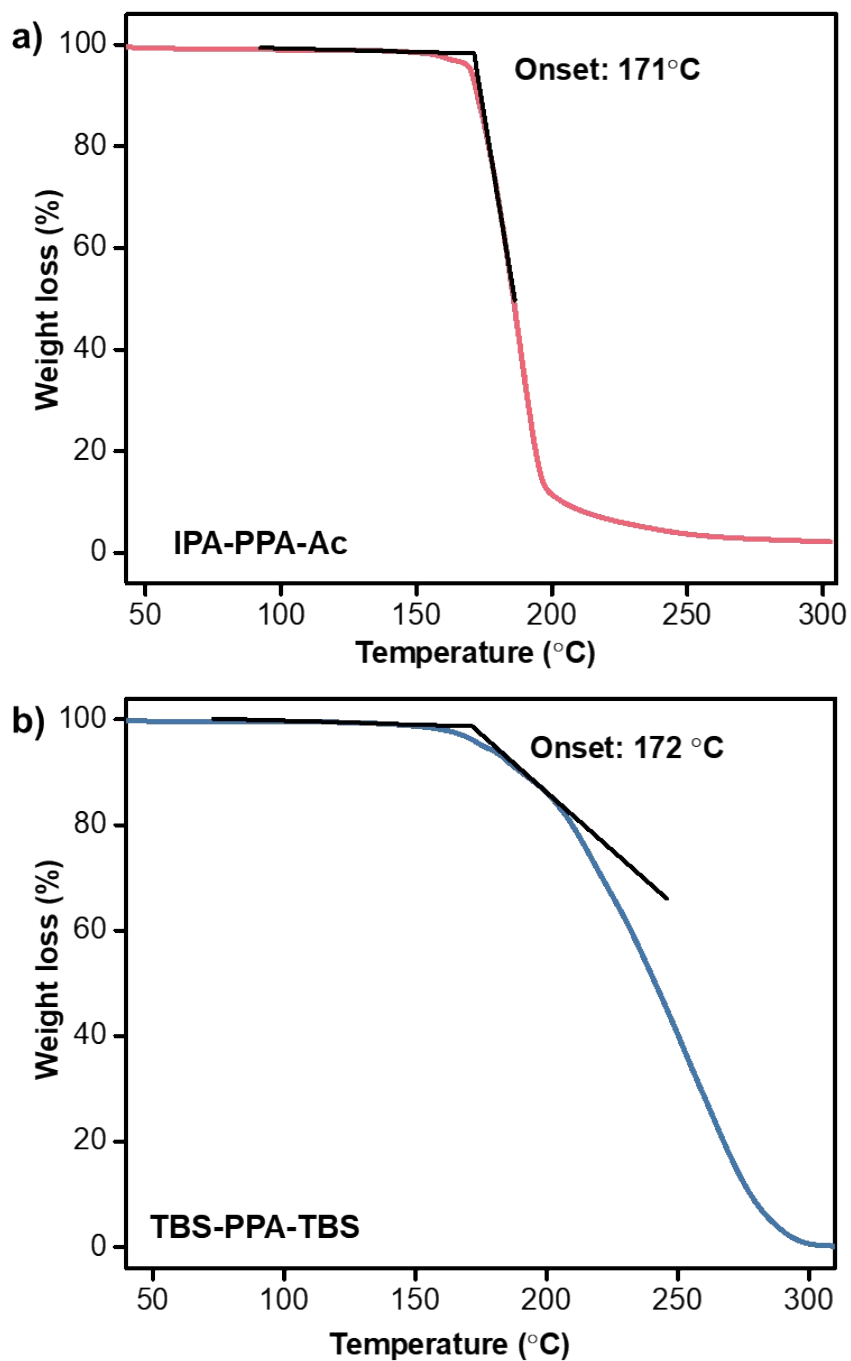


Figure S7. TGA curves of a) IPA-PPA-Ac and b) TBS-PPA-TBS along with the decomposition temperature of each polymer.

3.4. Differential scanning calorimetry (DSC)

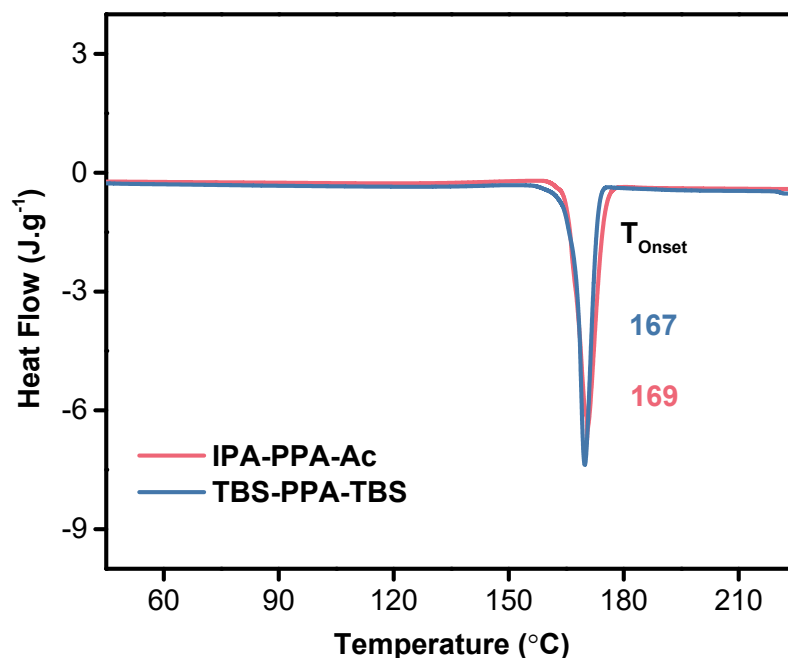


Figure S8. DSC plots of the synthesized PPA polymers along with the melting point of each.

4. Mechanical shearing strength of PPA

4.1 Solvent-assisted bonding of glass substrates

A solvent-assisted bonding process was used to bond smooth glass slides with PPA polymers for shear testing experiments. Initially, the glass slides were washed with water, ethanol, and acetone respectively to remove any contaminants found on the slides and to ensure that failure in the testing process is only due to adhesion/cohesion from the polymeric materials. After leaving the glass slides for 1 hour to dry on the bench, their masses and thicknesses were measured in accordance with the ASTM D-1002-10 standard. The polymeric solution was prepared by adding 100 mg of the PPA polymer into a 1 mL solution of methanol (MeOH) in a 4 mL vial forming a white cloudy suspension. The solution was then vortexed for 30 secs, followed by drop casting 0.1 mL of it (containing approximately 10 mg of the polymer) on each slide for a total of 10 glass slides. After the slides were allowed to dry for 30 mins, a minimal amount of dichloromethane (DCM) was added to dissolve the polymer, and immediately, complementary

clean glass slides were placed on top, such that the overlap area of the substrates was approximately at 20% of the length of the bottom slide initially containing the polymer. A 250 g stainless steel cylinder was placed on top of the assembly for 1 hour in an attempt to flatten the assembly, remove excess solvent, and improve surface wetting. Finally, the assemblies were placed in a vacuum chamber overnight at room temperature and at a pressure of 300 mtorr to remove excess solvent (MeOH and DCM) that may influence shear strength. The assemblies were removed from the vacuum chamber after 24 hr and cleaned with a razor blade to remove polymer residuals outside the adhesive area. Finally, the thickness and mass of each assembly were measured, and optical images of the assemblies were taken to quantify the overlap area and bonded area prior to shearing, which was accomplished using ImageJ 5.0.

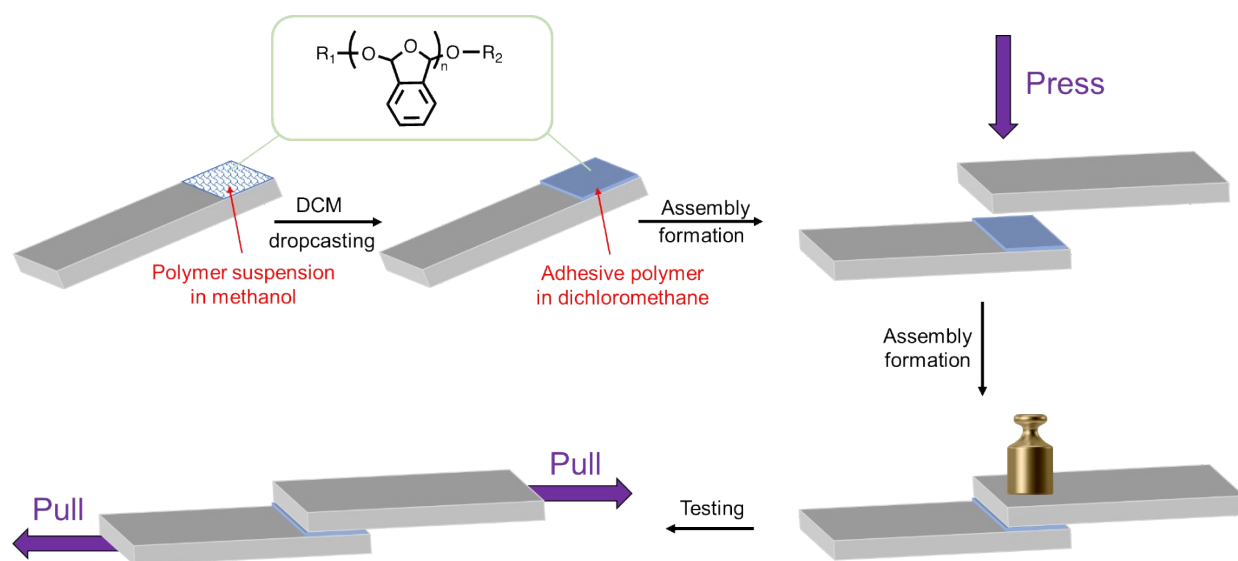


Figure S9. Preparation of glass bonded assemblies with linear PPA using the solvent-assisted bonding method.

4.2 Shear testing of bonded assemblies for adhesive characterization

A single column tensile tester (Instron 5544) was used to characterize the previously prepared assemblies and determine their lap shear properties. In brief, glass assemblies were placed into the two clamps of the shear testing instrument (one clamp holding the bottom slide while the other clamp holding the other slide) with the bottom substrate pointed down and sheared at a loading rate of 30 N.min⁻¹. Data obtained from this experiment portrays the maximum force that the assemblies can withstand before shearing (breaking) as a function of the extension. A typical

load/extension graph of the raw data obtained from a single lap shear test for IPA-PPA-Ac between two microscope glass slides is given in **Figure S11**. The profile includes three major segments. The beginning phase of a lap shear test shows a non-smooth area where the relation between load and displacement is non-linear, and the slope remains unchanged at zero despite a slight displacement. In this phase, the clamps of the Instron are stretching out, and hence the obtained data can be ignored. After the clamps settle into their final grip position, the inelastic loading phase begins where the force applied (in N) increases with displacement (in mm) until both slides in the assembly detach abruptly and the force load disappears. The location of the breakdown corresponds to the “failure point” and is, by definition, the maximum load that the material can endure before experiencing failure. Since the area of adhesion in all assemblies cannot be well controlled, we opted to calculate the lap shear strength of the assemblies, which is the ratio of the maximum force withstood before the overlap joint failed, to the area of the adhesive layer in the overlap joint:

$$\text{shear strength} = \frac{\text{Load (N)}}{\text{adhesive area}} \text{ (Equation S4)}$$

Where the adhesive area was measured using ImageJ.

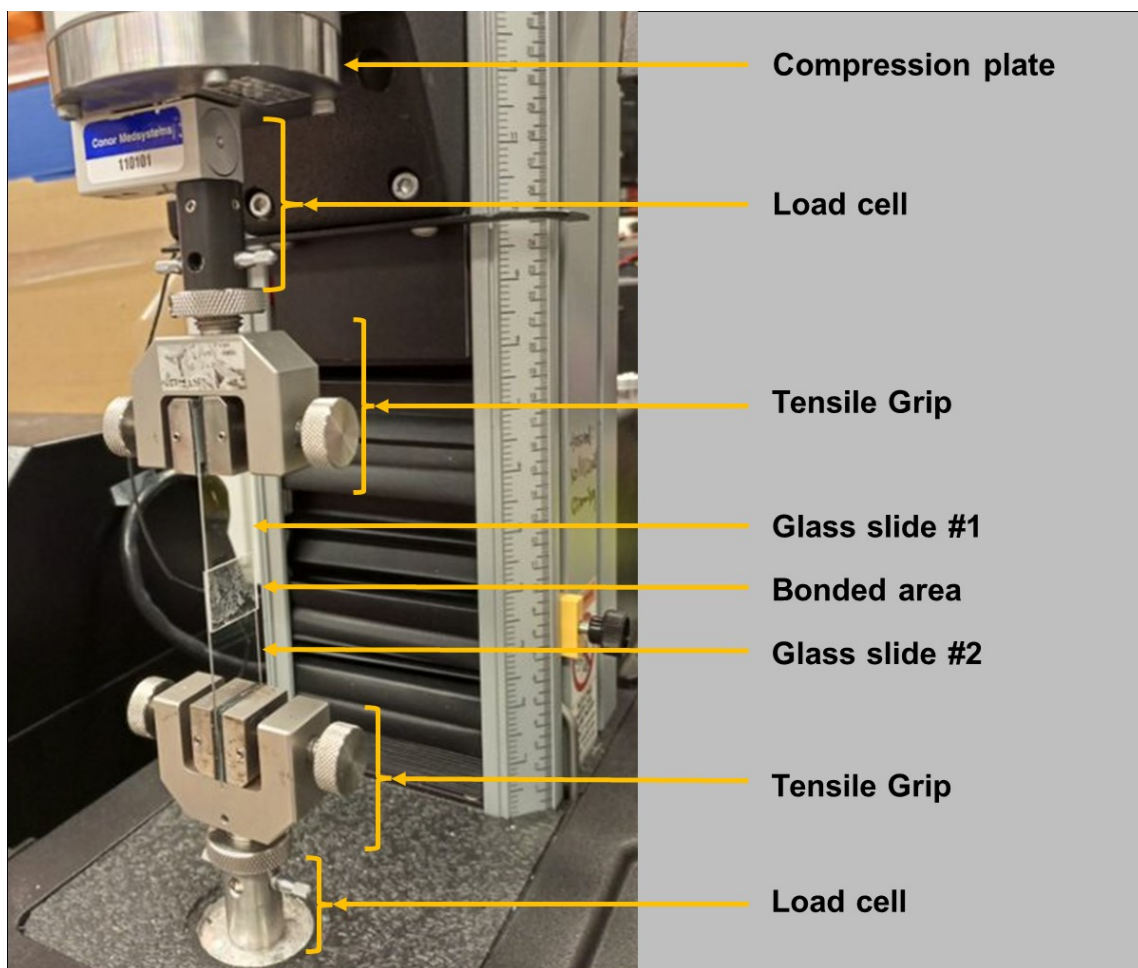


Figure S10. A glass assembly bonded by TBS-PPA-TBS placed into the two clamps of the shear testing instrument (Instron 5544) before testing. 500N load cells were used throughout all experiments.

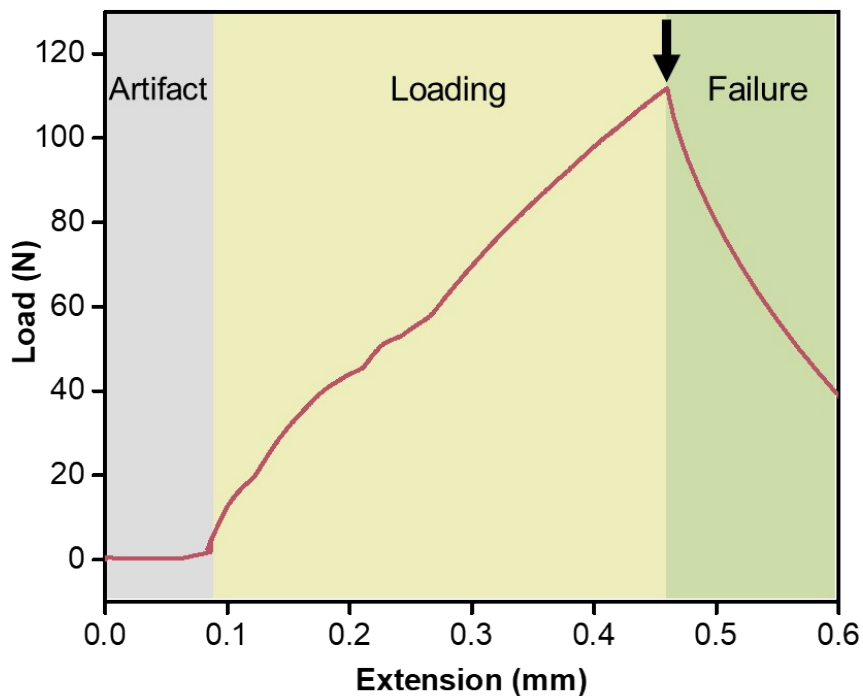


Figure S11. A representative graph of the raw data from a lap shear test for IPA-PPA-Ac between two microscope glass slides. The arrow points to the “failure point”.

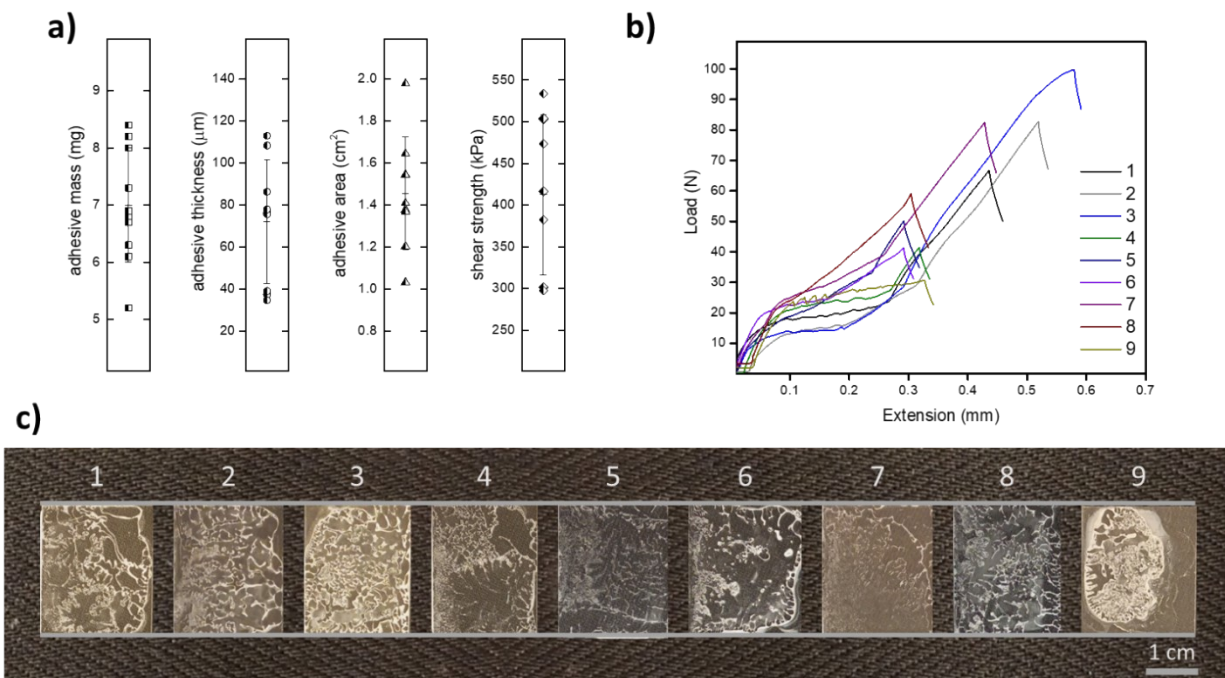


Figure S12. a) Adhesion and shearing strength data of IPA-PPA-Ac without plasticizer. b) Load vs. Extension plot of all IPA-PPA-Ac samples. c) Pictures of the respective samples of IPA-PPA-Ac adhesives.

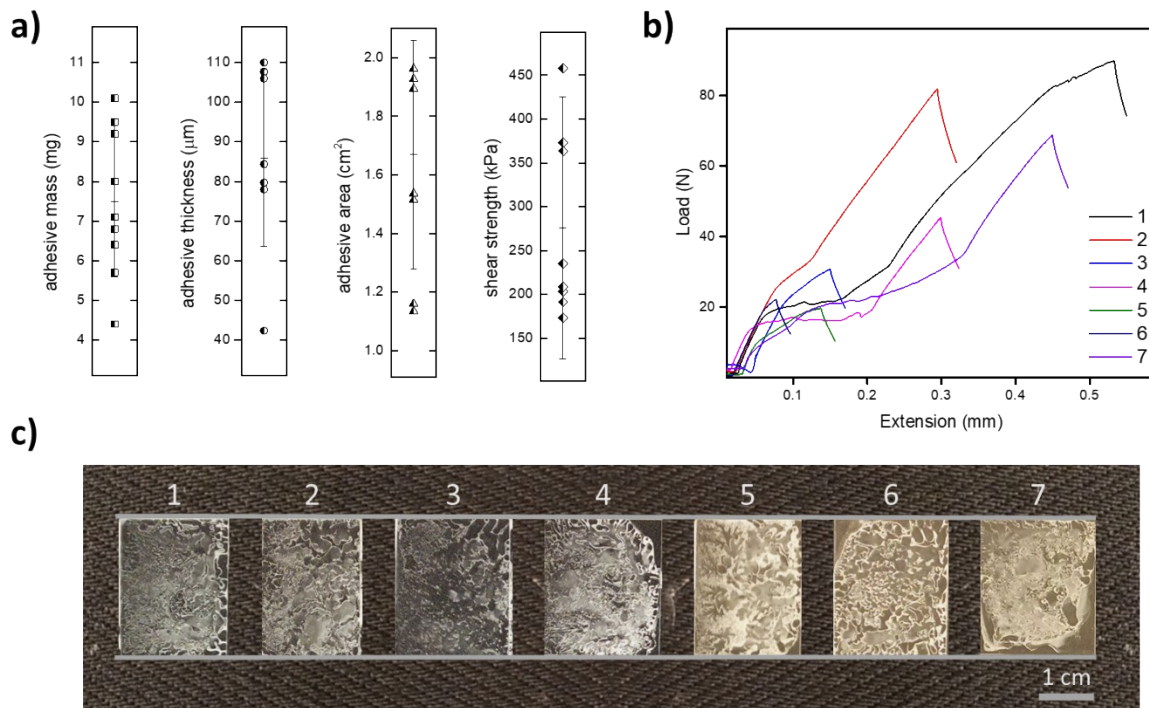


Figure S13. a) Adhesion and shearing strength data of TBS-PPA-TBS without plasticizer. b) Load vs. Extension plot of all TBS-PPA-TBS samples. c) Pictures of the respective samples of TBS-PPA-TBS adhesives.

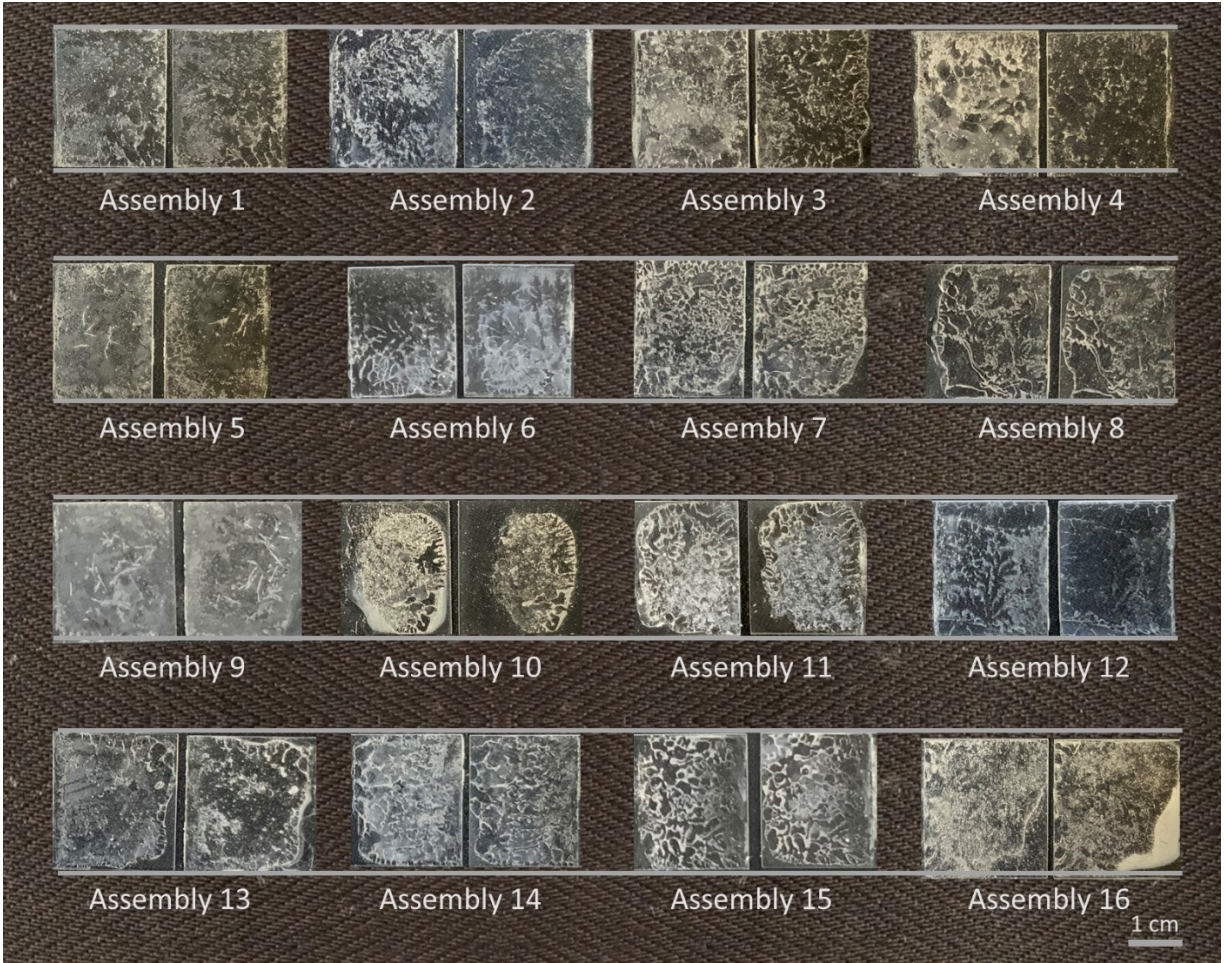


Figure S14. Smooth glass bonded slides with PPA after shearing. Note how discrete islands of PPA appear on all slides indicating a mixed cohesive/adhesive failure predominant by cohesion.

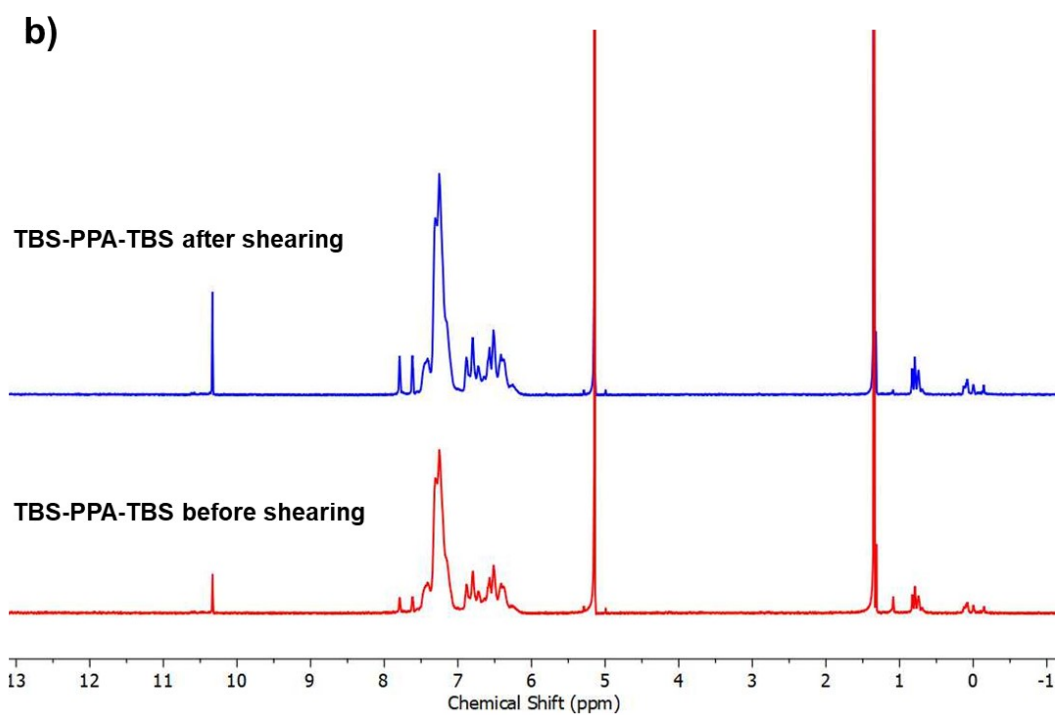
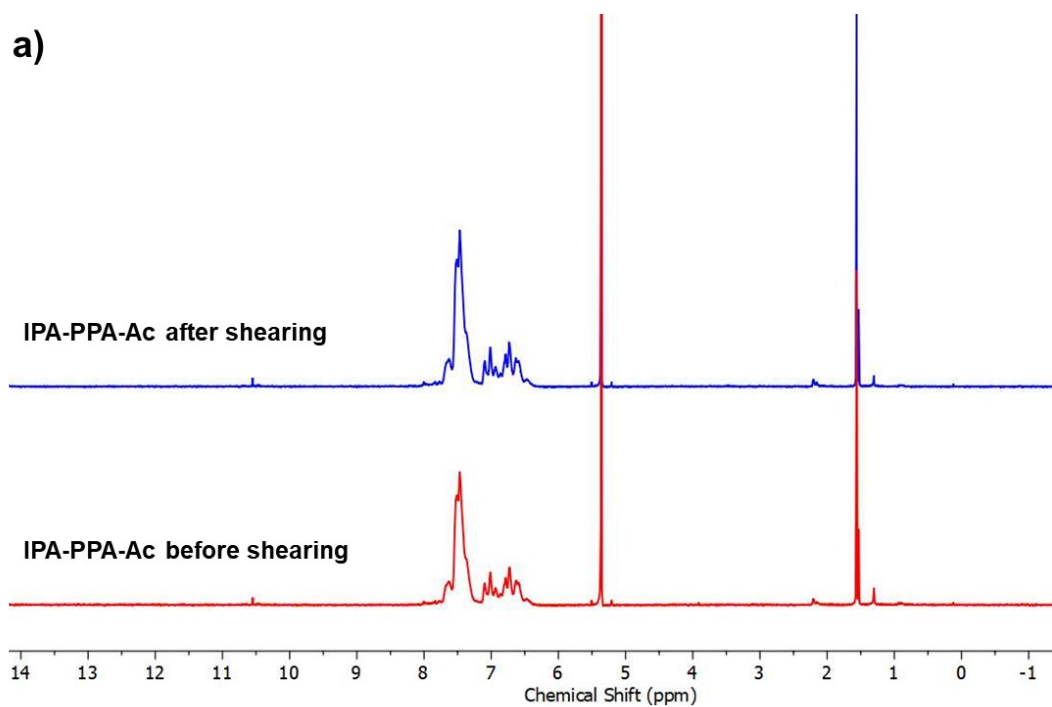


Figure S15. $^1\text{H-NMR}$ spectra of a) IPA-PPA-Ac and b) TBS-PPA-TBS before and after shear tests in DCM.

Purity of PPA rel. to O-PA		
Polymer sample	Before shearing	After shearing
IPA-PPA-Ac	99.1 %	98.9 %
TBS-PPA-TBS	98.0%	96.3 %

Table S2. The purity of PPA samples relative to the starting monomer before and after shear testing. Calculations were carried out based on the integration curves of the monomer and polymer peaks using equation S1.

4.3 Melt bonding of substrates with poly(phthalaldehyde)/plasticizer material

A melt bonding process was used to bond smooth glass slides with a homogeneous mixture of PPA polymer and DMP plasticizer for shear testing experiments. Initially, the glass slides were washed with water, ethanol, and acetone to remove any contaminants found on the slides and to ensure that failure in the testing process is solely attributed to adhesion/cohesion from the polymeric materials and not contaminants on the glass slides. After leaving the glass slides to dry for 1 hr on the bench, their masses and thicknesses were measured in accordance with the ASTM D-1002-10 standard. The polymeric solution was prepared by dissolving 100 mg of the PPA polymer in 0.98 mL of DCM in a 4 mL vial. After sonication for a few seconds, 16.8 μ L of DMP solution were added to the previously prepared polymer solution and the mixture was vortexed for 30 seconds resulting in a 20% (w/w) DMP/PPA solution. A small amount of the solution (0.1 mL) was drop-casted onto the cleaned slides for a total of 10 glass slides and allowed to dry for 15–30 min. Clean glass slides were later placed on top such that the overlap area of the substrates was approximately 10% the length of the bottom slide initially containing the polymer. Immediately the assemblies were heated on a hot plate at 80°C to remove excess solvent and transform the polymer from its brittle state into a rubbery state. Finally, the assemblies were left to cool on the bench for a few minutes and then placed in a vacuum chamber at room temperature overnight at a pressure of 300 mtorr to remove excess solvent (MeOH and DCM) that may influence shear strength. The assemblies were removed from the vacuum chamber after 24 hrs and cleaned with a razor blade to remove polymer residuals outside bonded area. Finally, the thickness and mass of each assembly was measured, and optical images of the assemblies were also taken to quantify the overlap area and bonded area prior to shearing, which was accomplished using ImageJ 5.0.

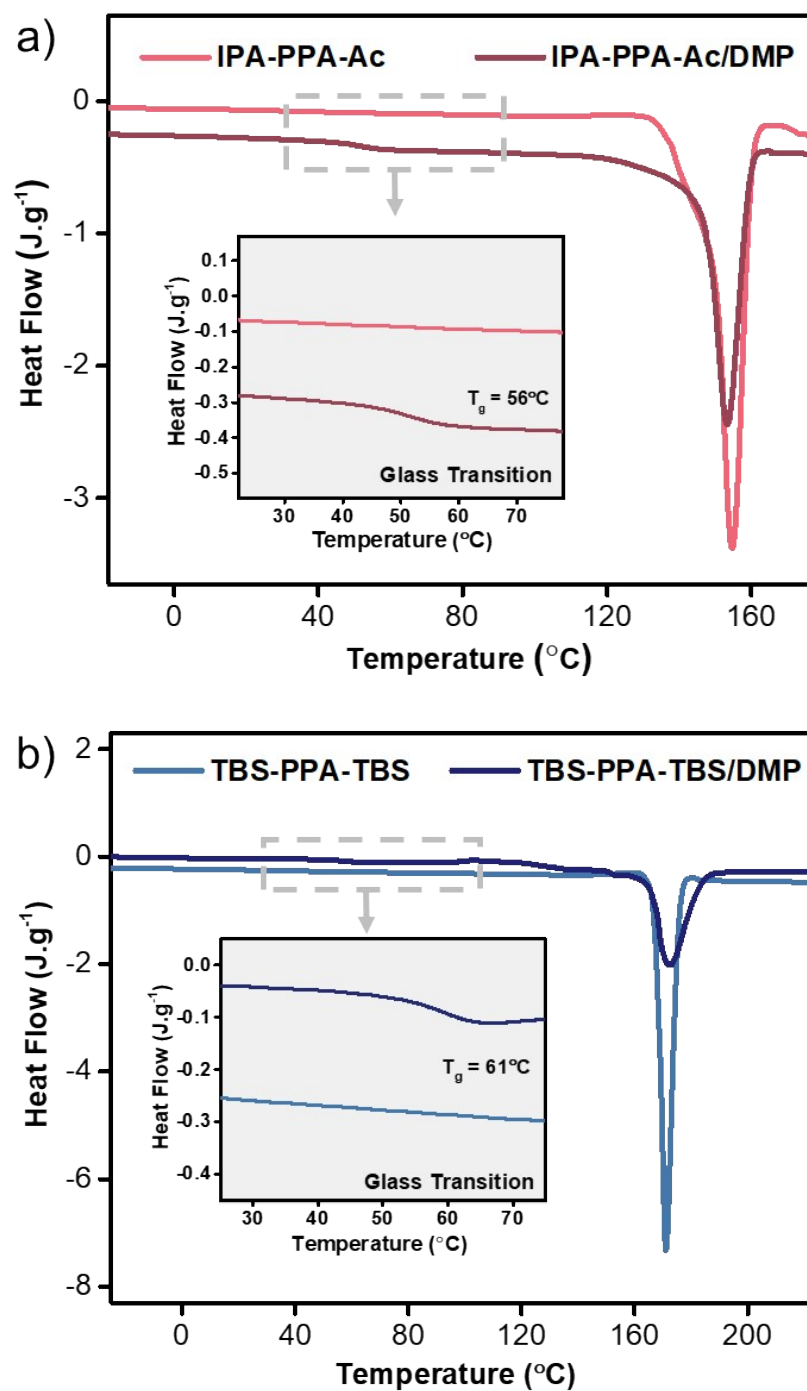


Figure S16. a) Overlaid DSC thermograms of IPA-PPA-Ac without DMP (cyan) and with 20% (w/w) DMP plasticizer (Cobalt Blue). Inset expands glass transition region; and b) Overlaid DSC thermograms of TBS-PPA-TBS without DMP (Lawn green) and with 20% (w/w) DMP plasticizer (Olive). Inset expands glass transition region.

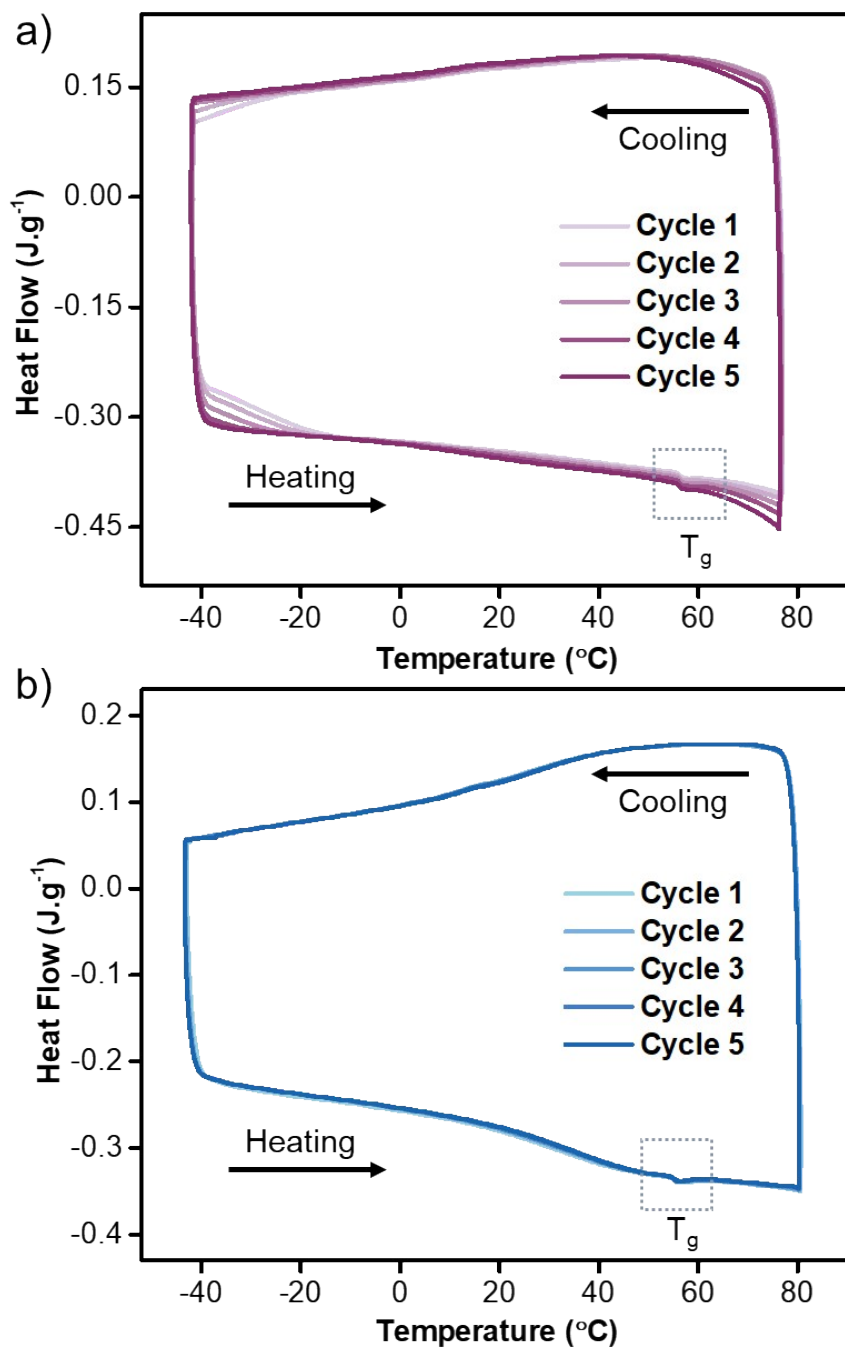


Figure S17. DSC thermal cycling experiments on a) IPA-PPA-AC/DMP and b) TBS-PPA-TBS/DMP confirming the robustness of the plasticized materials.

4.4 Shear testing of PPA/DMP bonded assemblies for adhesive characterization

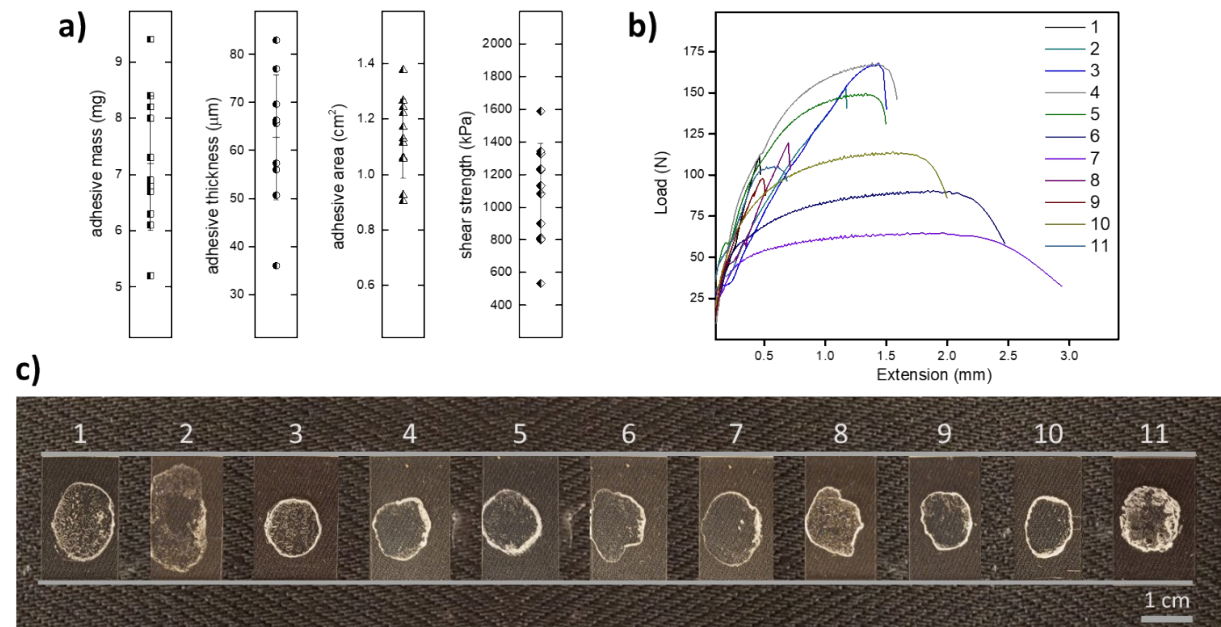


Figure S18. a) Adhesion and shearing strength data of IPA-PPA-Ac with plasticizer. b) Load vs. Extension plot of all samples of IPA-PPA-Ac with plasticizer. c) Pictures of the respective samples of IPA-PPA-Ac adhesives with plasticizer.

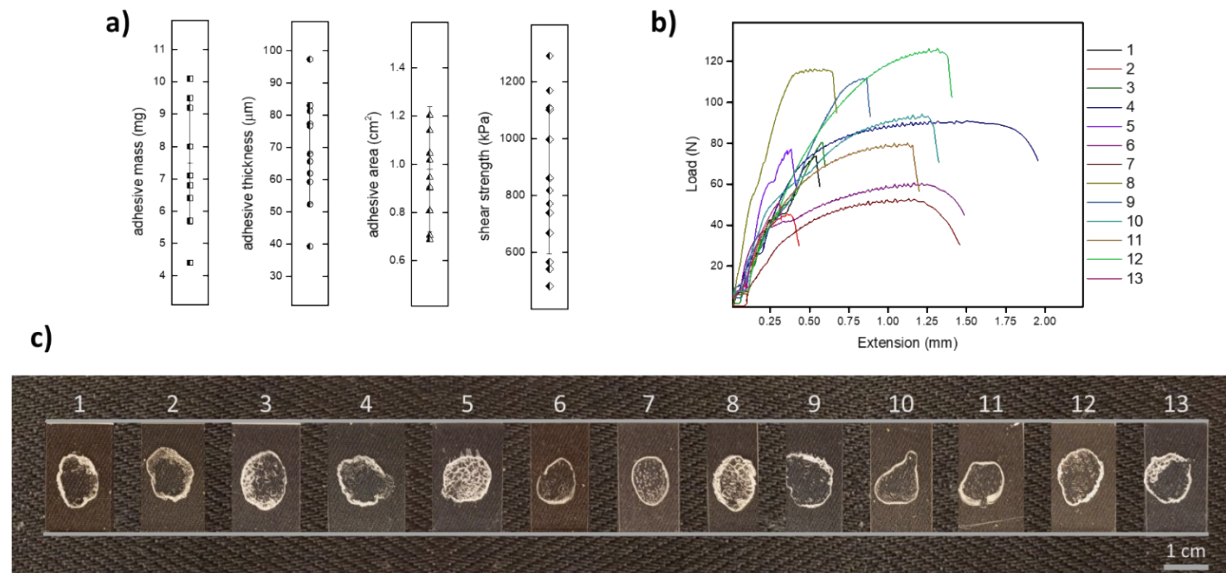


Figure S19. a) Adhesion and shearing strength data of TBS-PPA-TBS with plasticizer. b) Load vs. Extension plot of all samples of TBS-PPA-TBS with plasticizer. c) Pictures of the respective samples of TBS-PPA-TBS adhesives with plasticizer.

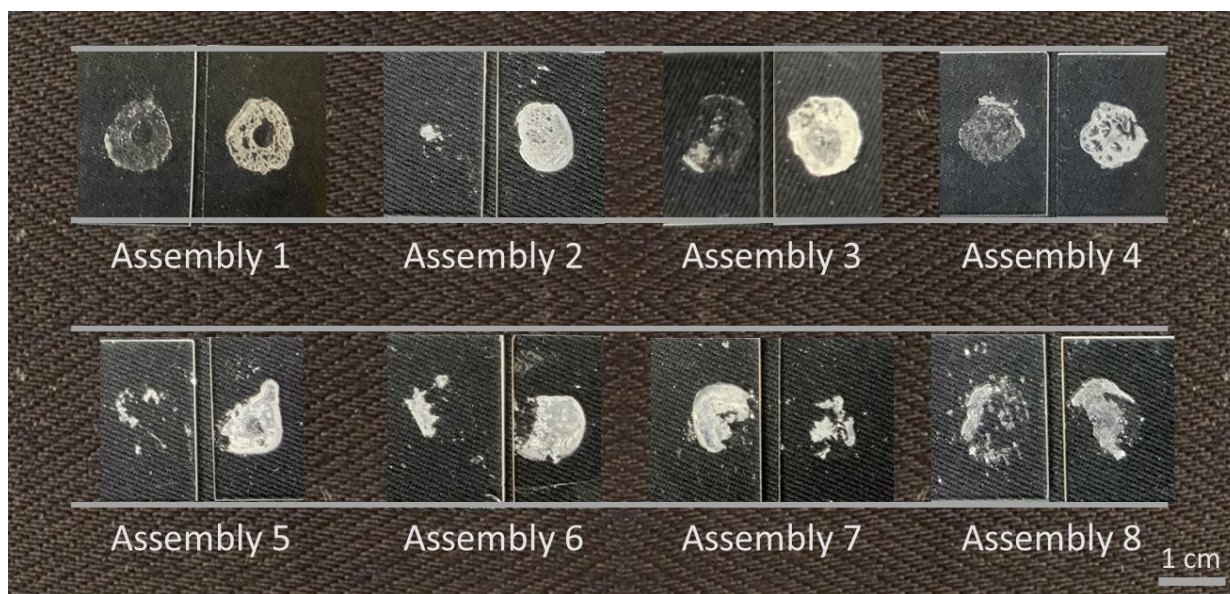


Figure S20. Representative smooth glass bonded slides with PPA /DMP after shearing. Note how discrete the polymer/plasticizer blends are remaining only on one glass slide of the assembly indicating a strong adhesion mode of failure.

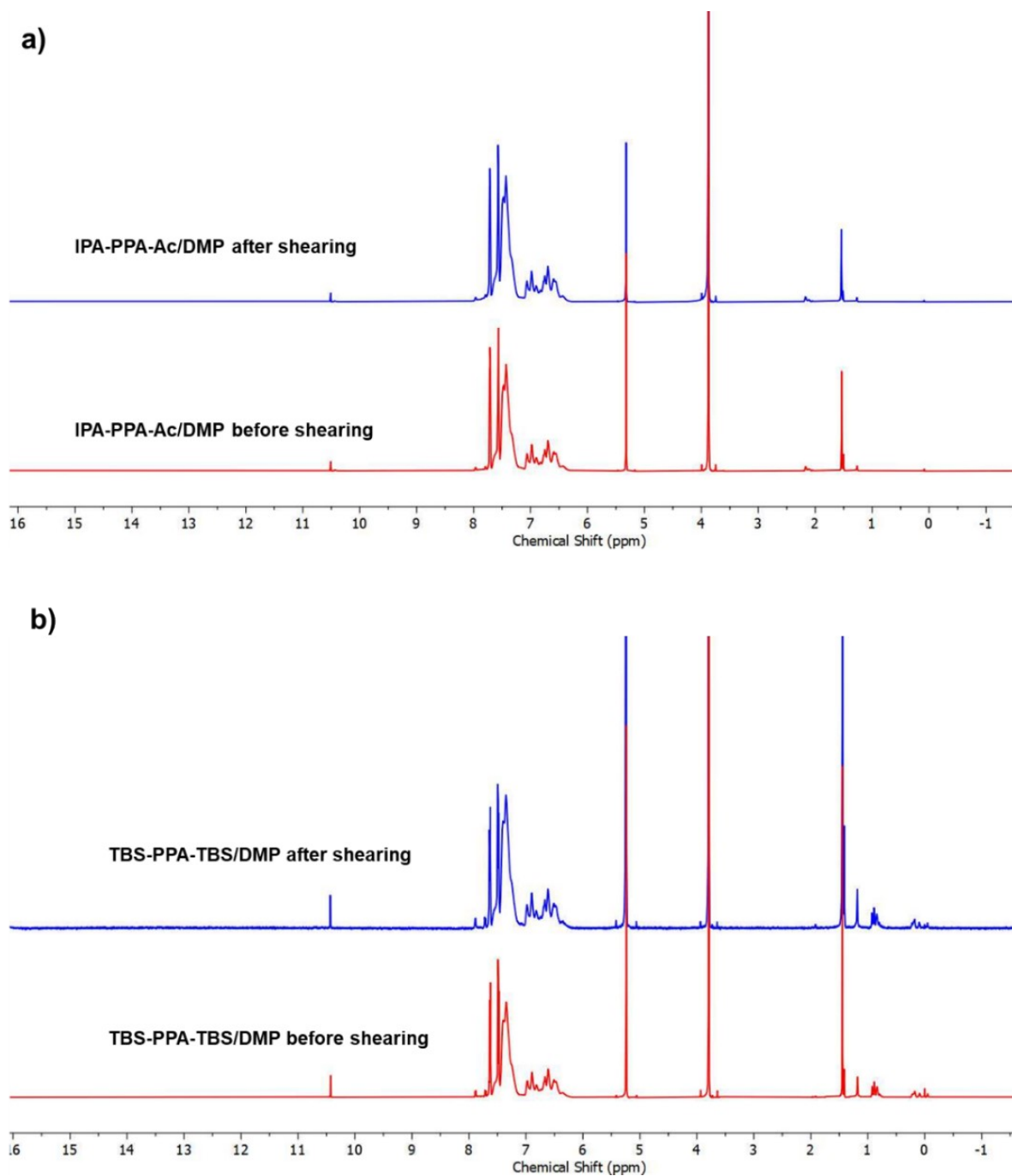


Figure S21. $^1\text{H-NMR}$ spectra of a) IPA-PPA-Ac/DMP and b) TBS-PPA-TBS/DMP before and after shear tests. Note that the peaks appearing at 3.8, 7.5 and 7.6 ppm correspond to the DMP plasticizer.

5. Acid triggered depolymerization of PPA

5.1. Acid-triggered depolymerization of IPA-PPA-Ac

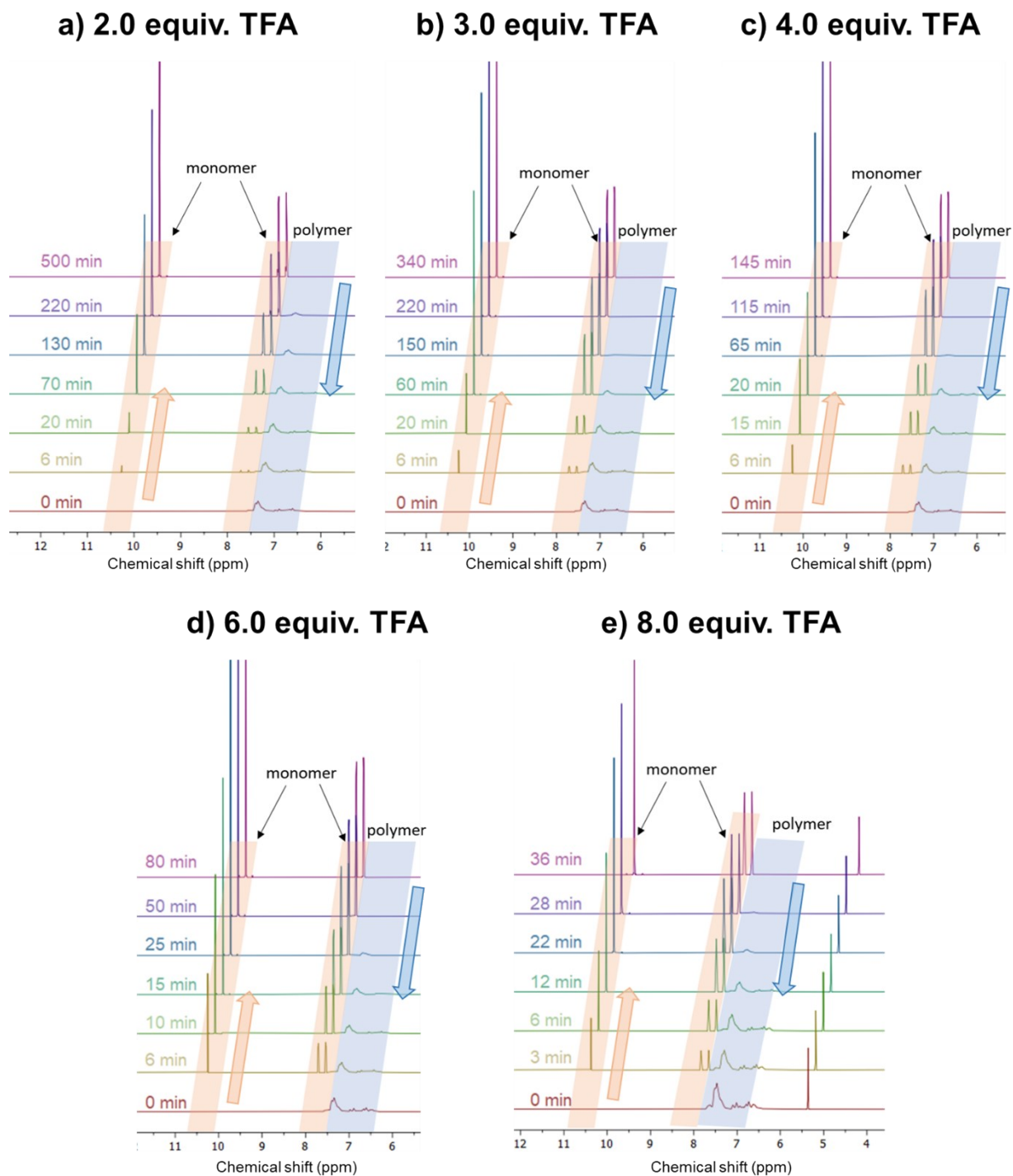


Figure S22. The variation in the ^1H -NMR spectra of IPA-PPA-Ac upon exposure to various doses of TFA at different time intervals.

5.2. Integrated rate laws

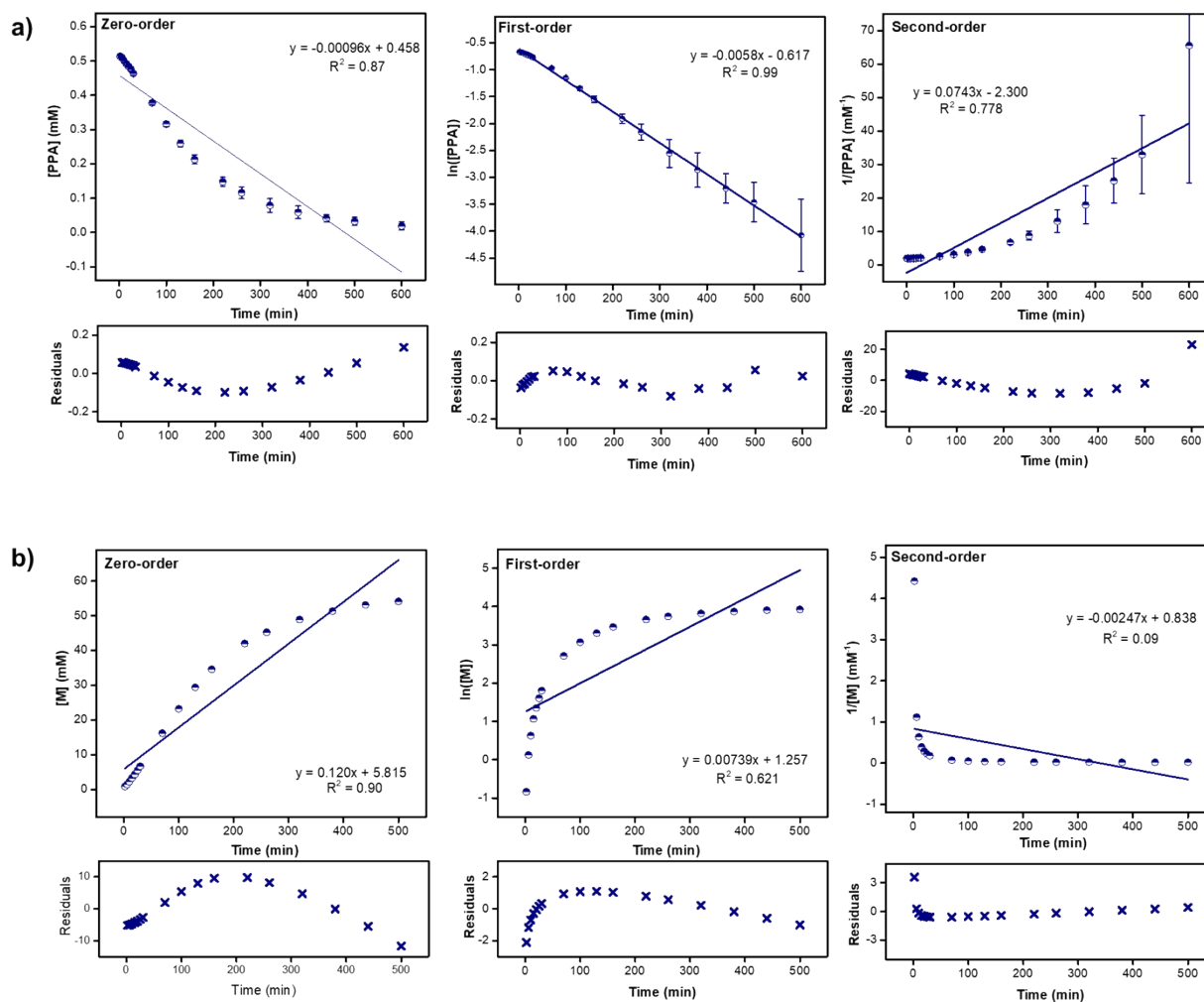


Figure S23. Kinetic study of IPA-PPA-Ac depolymerization according to a) polymer and b) monomer. Zero-order, first-order, and second order plots of the depolymerization at 2 equiv. of TFA.

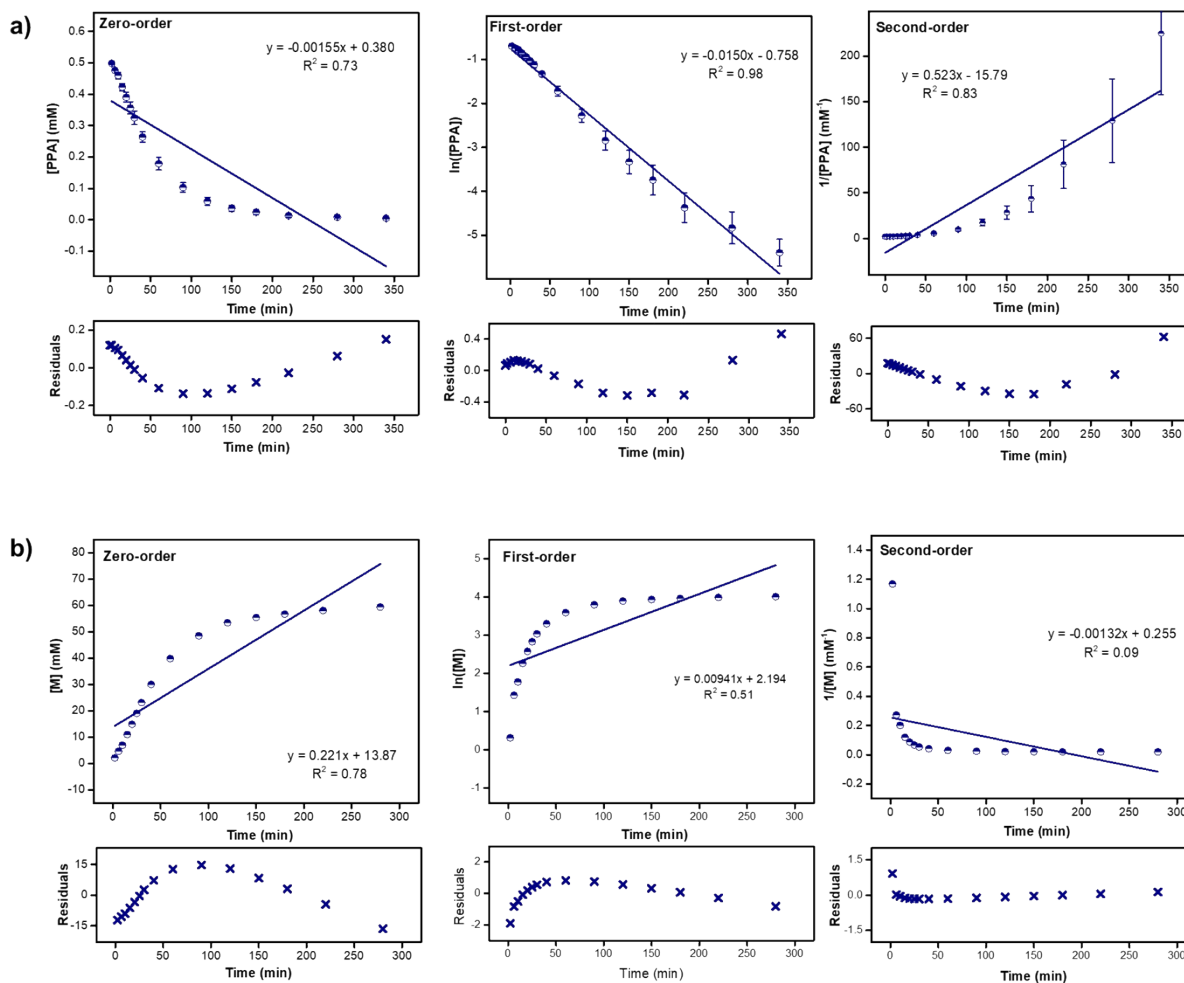


Figure S24. Kinetic study of IPA-PPA-Ac depolymerization according to a) polymer and b) monomer. Zero-order, first-order, and second order plots of the depolymerization at 3 equiv. of TFA.

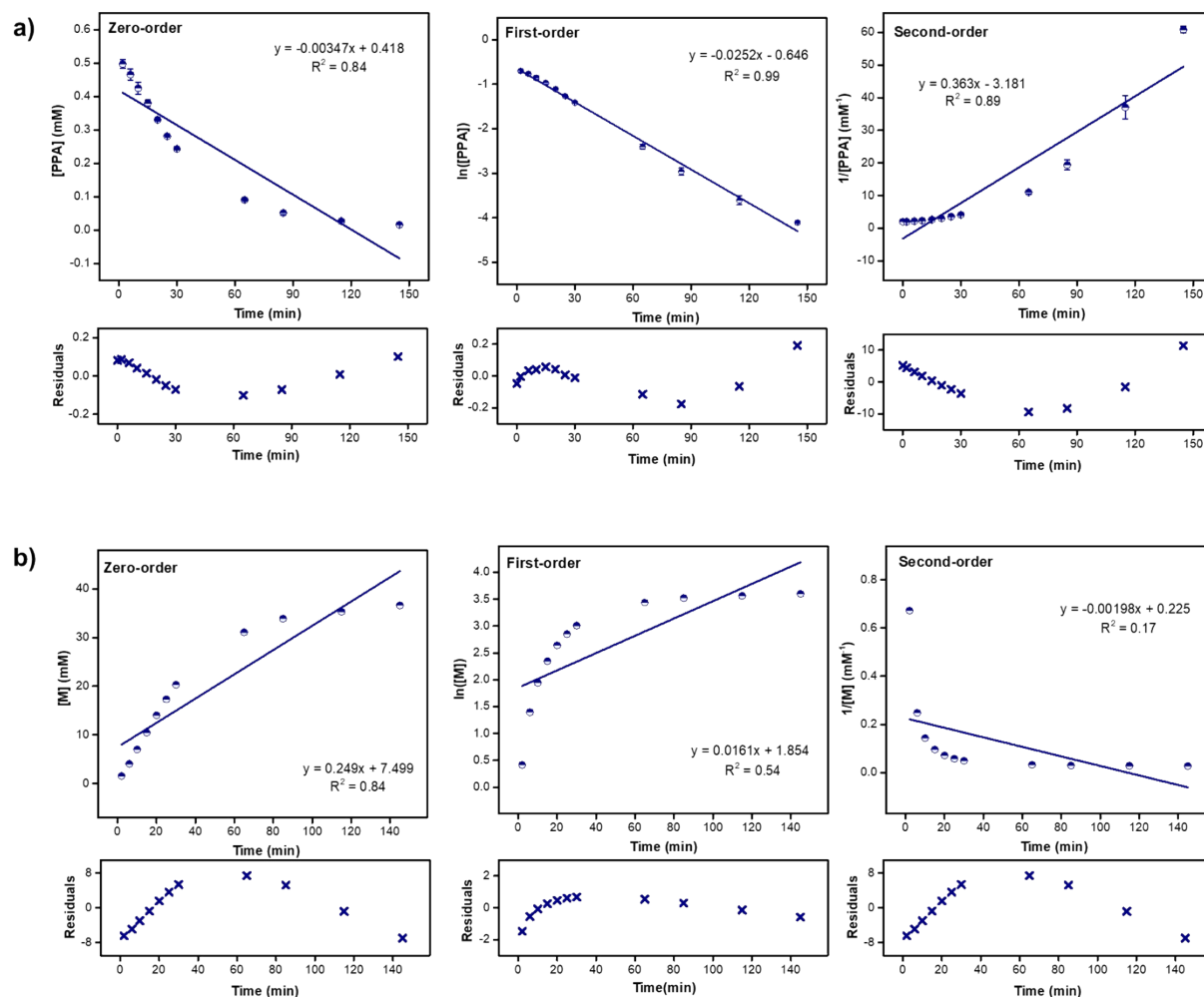


Figure S25. Kinetic study of IPA-PPA-Ac depolymerization according to a) polymer and b) monomer. Zero-order, first-order, and second order plots of the depolymerization at 4 equiv. of TFA.

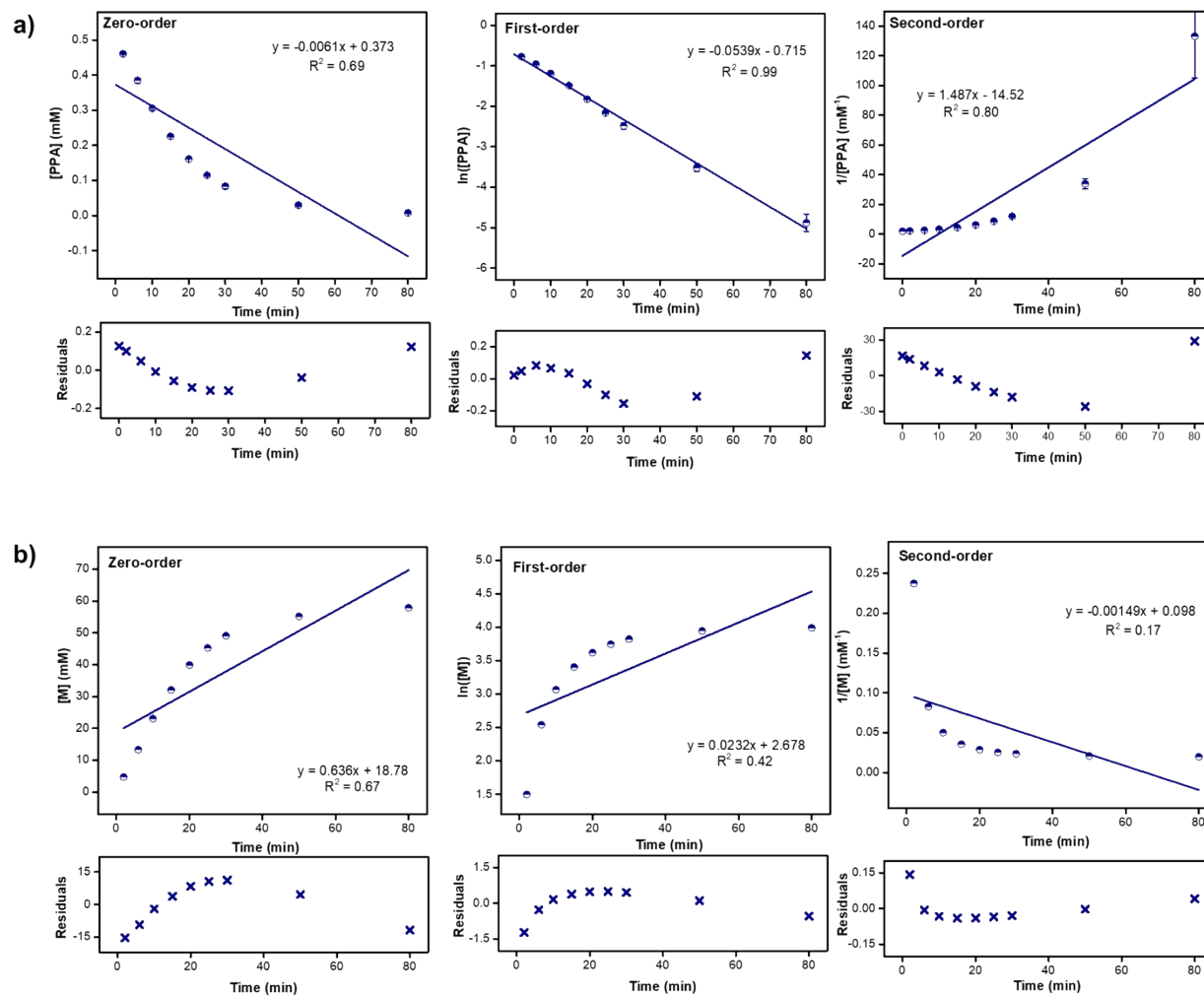


Figure S26. Kinetic study of IPA-PPA-Ac depolymerization according to a) polymer and b) monomer. Zero-order, first-order, and second order plots of the depolymerization at 6 equiv. of TFA.

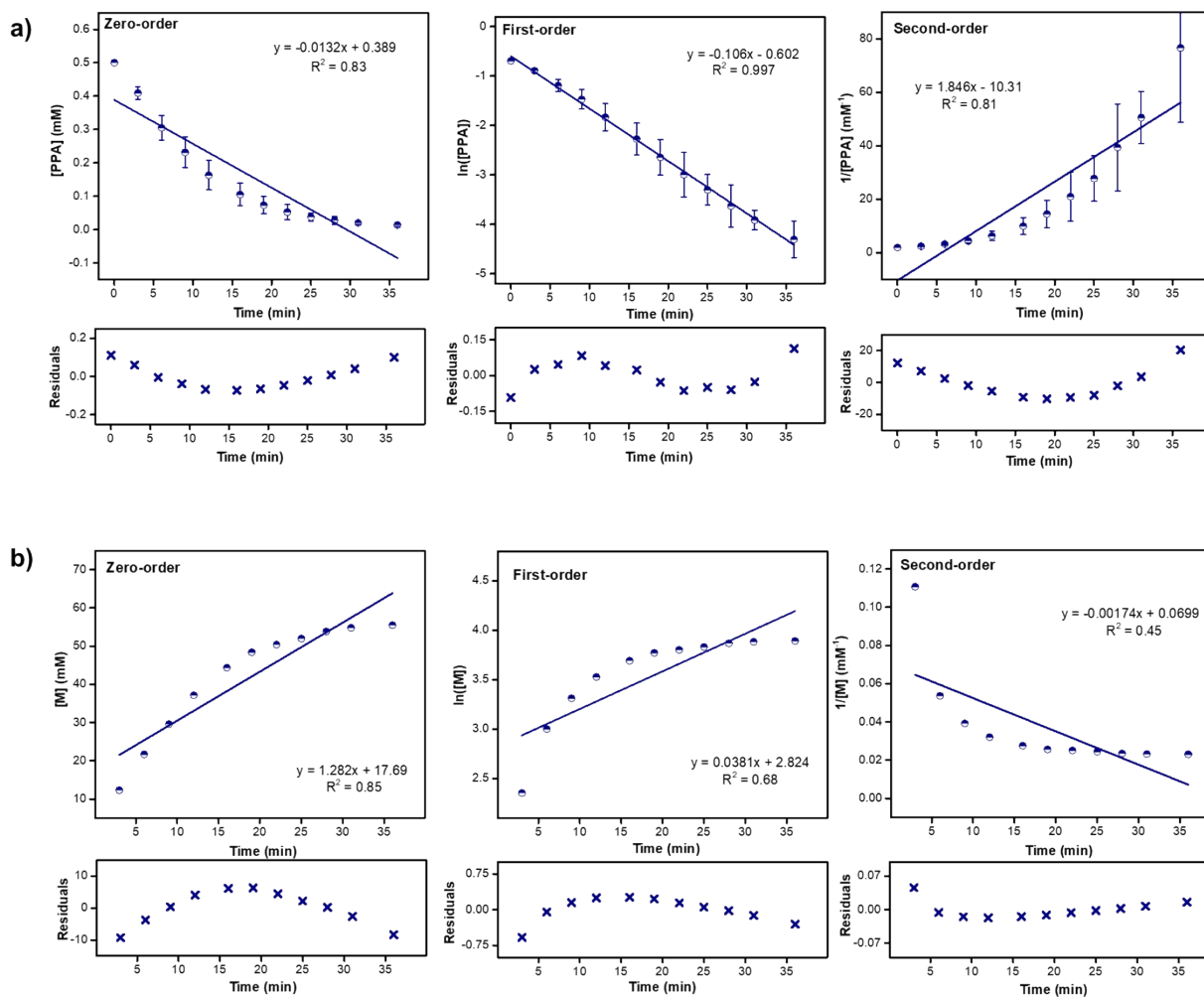


Figure S27. Kinetic study of IPA-PPA-Ac depolymerization according to a) polymer and b) monomer. Zero-order, first-order, and second order plots of the depolymerization at 8 equiv. of TFA.

5.3. Residual plots significance

Overall, different types of residual plots exist, which are utilized to determine whether the applied linear regression model is appropriate to represent the data.¹ For a regression function to be linear and preferred, the residuals ought to bounce randomly around the identity line to form a null residual plot.² Interestingly, a positive serial correlation in the data error terms was observed for PPA, especially for the pseudo-first order plots where residuals tend to be followed, in time, by residuals of the same sign in what appears to be a continuation of the first cycle. Hence, the

assumption of independent error terms in this case is violated and neither of the three linear models is adequate to describe the mechanism of the acid-triggered depolymerization of PPA.

5.4 Cationic polymerization for the generation of cyclic poly(phthalaldehyde)

5.4.1 Synthesis of cyclic poly(phthalaldehyde) (cPPA)

Cyclic PPA was generated via a procedure reported in the literature with some modifications.³ In brief, 1.3 g of *o*-PA monomer (9.7 mmol) was added to an oven-dried 50 mL RDF charged with a PTFE magnetic stirring bar under argon atmosphere. 13 mL of anhydrous DCM were then added via a disposable needle under positive pressure and the resulting solution was allowed to stir under argon for an additional 30 mins to ensure an air-free environment and to avoid monomer oxidation. The solution was cooled down to -78°C followed by the addition of 30 μL boron trifluoride etherate (0.24 mmol) to initiate polymerization. The resulting mixture was allowed to stir for 3 hours before being quenched with 0.16 mL of pyridine. After allowing the solution to stir for an additional 2 hours, it was brought to room temperature over a period of 1 hour followed by precipitating the resulting product in 130 mL of MeOH. The resulting white powder was collected by filtration, then purified by dissolving it in 7 mL of DCM and adding it dropwise to 70 mL of MeOH, allowing its precipitation to afford a white polymeric material (1.16 g, 92% yield).

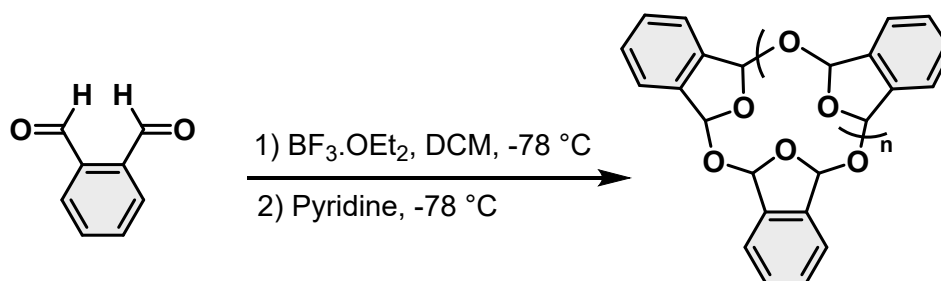


Figure S28. Synthesis procedure of cPPA via a cationic polymerization process.

5.4.2 Spectroscopic characterization of cPPA

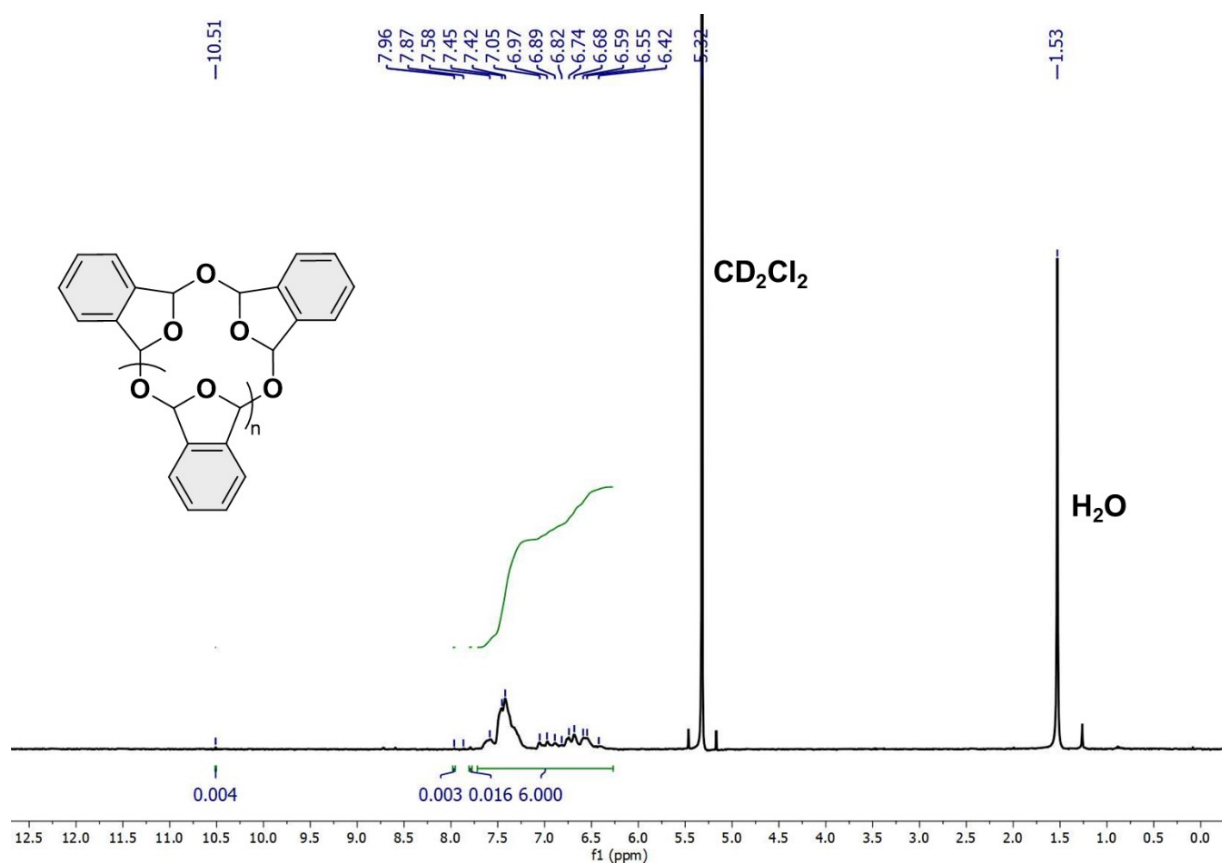


Figure S29. ¹H-NMR of cyclic PPA in CD₂Cl₂-d₂ at 600MHz. The purity of the polymer compared to *o*-phthalaldehyde was calculated based on Equation 1 to be 99.6%.

5.4.3 Chromatographic characterization of cPPA

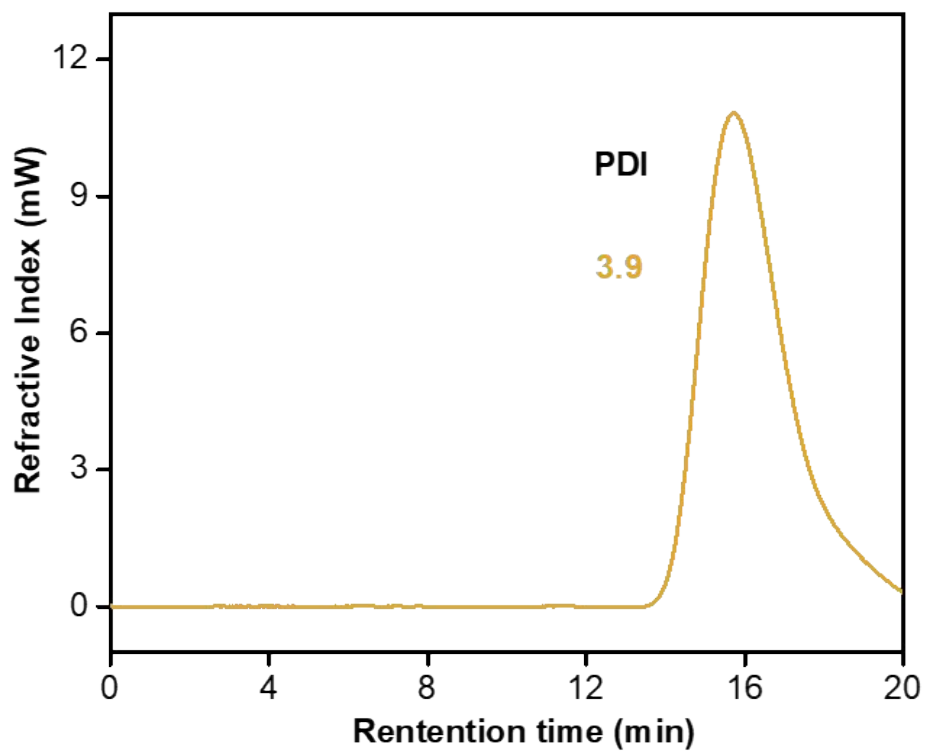


Figure S30. Representative GPC elution curve for cyclic PPA in DMF. Both the PDI and molecular weight distribution were determined after running a series of poly(styrene) standards in DMF.

5.4.4 Thermal characterization of cPPA

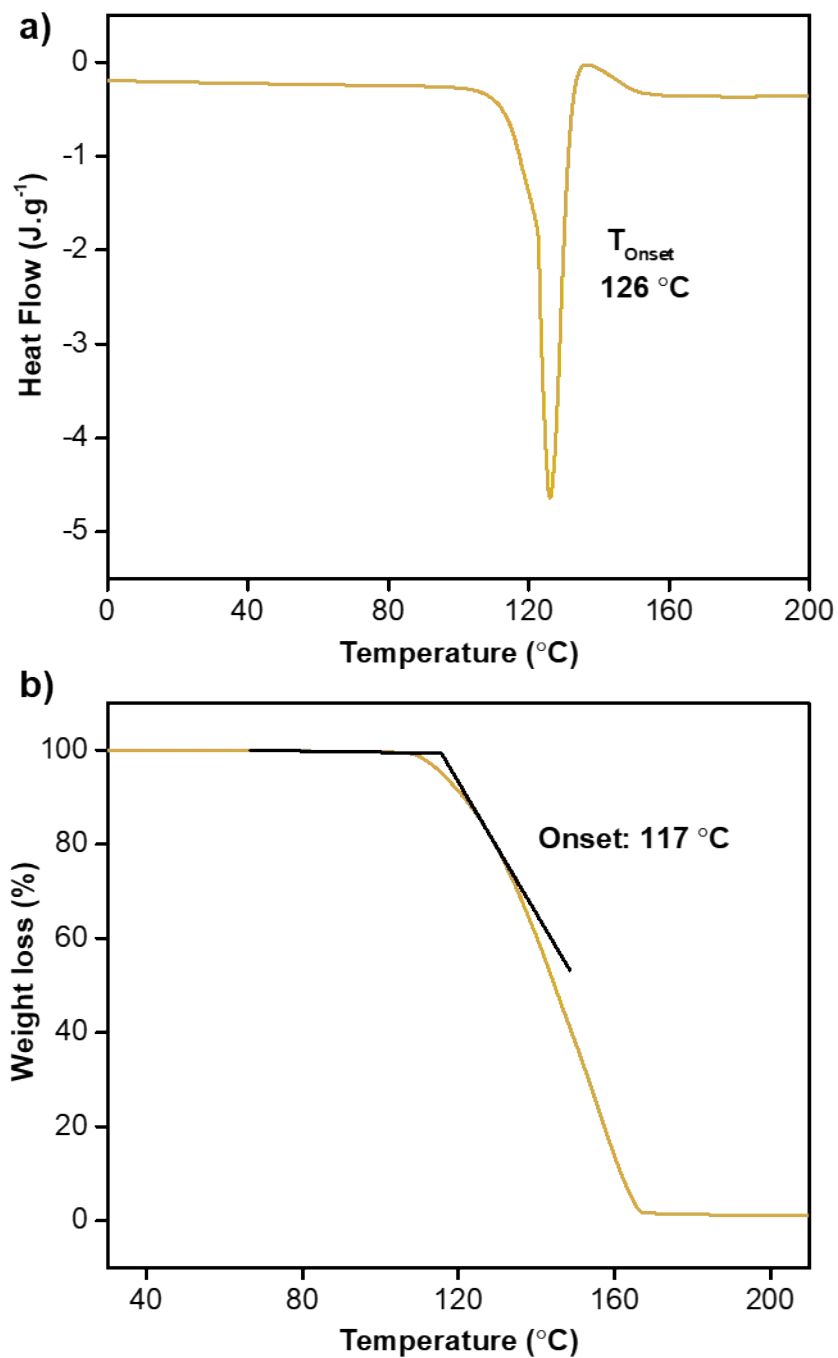


Figure S31. a) DSC plot of cyclic PPA along with its decomposition temperature and b) TGA curve of the polymer with its melting point.

Characterization technique	Properties	Cyclic PPA
$^1\text{H-NMR}$	Purity rel. to <i>o</i> -pa	99.6 %
GPC	Number Average Molecular Weight (M_n)	162.5 KDa
	Weight Average Molecular Weight (M_w)	626.2 KDa
	Polydispersity index	3.9
TGA	Decomposition temperature	117 °C
DSC	Melting point	126 °C

Table S3. Chemical and thermal properties of cyclic PPA generated via a cationic polymerization process.

5.5. Acid-triggered decomposition of TBS-PPA-TBS and *c*PPA

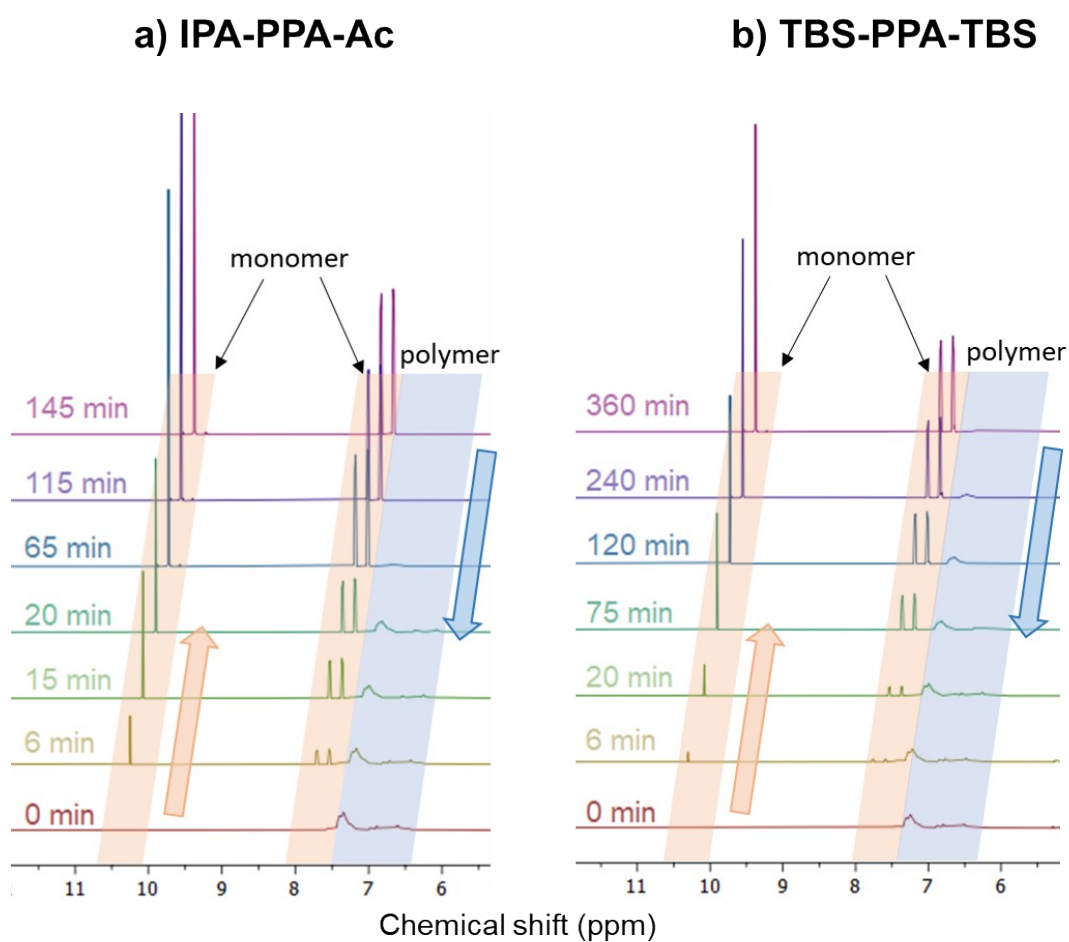


Figure S32. $^1\text{H-NMR}$ spectra of both PPA polymers after exposure to 4.0 equivalents of TFA.

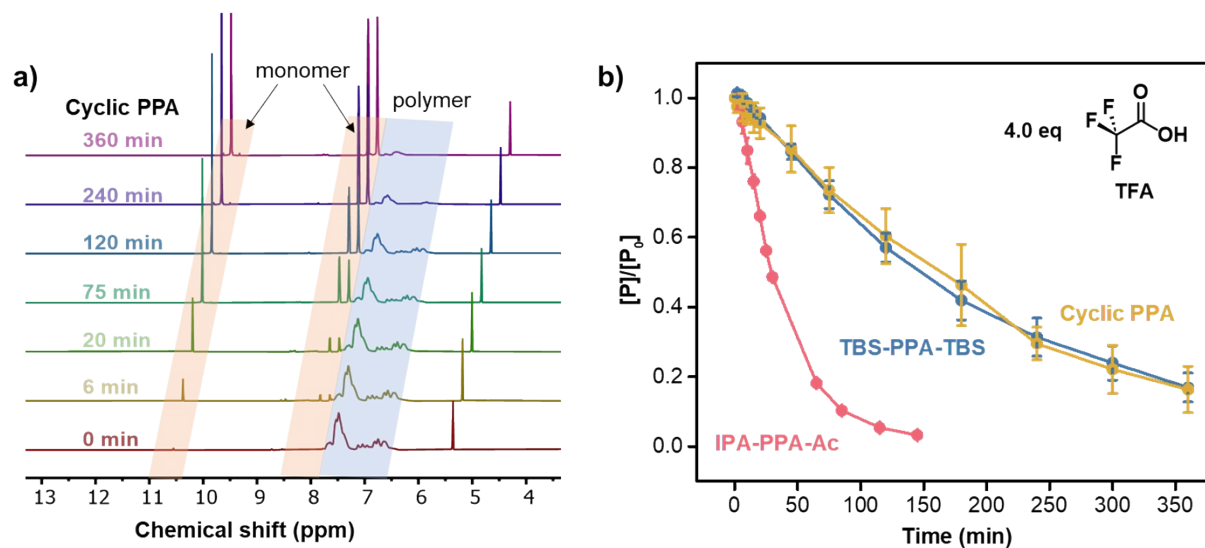


Figure S33. a) ¹H-NMR spectra cPPA after exposure to 4.0 equivalences of TFA and b) ratio of acid-triggered depolymerization with time of 0.5 mM of all synthesized poly(phthalaldehyde)-based polymers upon exposure to 4.0 equivalences of TFA (2.0 mM).

5.6 Overestimation of the molecular weight of PPA via GPC measurements

Based on the data presented in **Table S1**, we noted a discrepancy between the molecular weights (M.W.) of the polymers estimated via ¹H-NMR and GPC measurements. Throughout this study, we relied on the more accurate end-group analysis method by ¹H-NMR spectroscopy to determine the number-average molecular weights of IPA-PPA-Ac and TBS-PPA-TBS polymers. Through this absolute method, the ratio of the six protons in the repeating units of PPA to a specific proton in the end cap is calculated, which leads to the calculation of the number of repeating units in the polymer chain and eventually the overall M.W. of the polymer. However, cPPA is known to have no functional endcaps, which prevents the determination of its M.W. by ¹H-NMR. One viable method that has been extensively used in the literature to estimate the M.W. of cPPA in addition to some linear PPA polymers is GPC.⁴⁻⁶ This method separates macromolecules on the principle of the difference in their sizes and hydrodynamic volumes and hence relies on a specific pattern to determine the M.W. By running a series of primary standards with known M.W., followed by the construction of a primary calibration curve of logarithm of the molecular weight on the vertical axis and the retention volume on the horizontal axis, the M.W. of PPA can be estimated relative to the hydrodynamic volume of standards.⁷ Nonetheless, GPC often overestimates the true M.W. of polymers as is the case with PPA where we noticed a near 2-fold increase in the average number M.W. determined via GPC compared to the ¹H-NMR end group analysis method.⁸ One

of the reasons for this discrepancy can be attributed to the usage of monodisperse polystyrene (PS) polymers as primary standards rather than PPA standards since the latter is commercially unavailable. These polymers, despite having somehow similar repeating aromatic hydrocarbons, adopt a different conformation in solution, yielding results susceptible to analyte aggregation and stiffness.⁹ In addition, there exists no Mark-Houwink (M-H) parameters for PPA in the literature, which are crucial in converting the primary calibration curve constructed from PS into a universal curve able to correlate between the GPC curve of PPA and PS standards.

5.7. Mechanism of the acid-catalyzed degradation of IPA-PPA-Ac

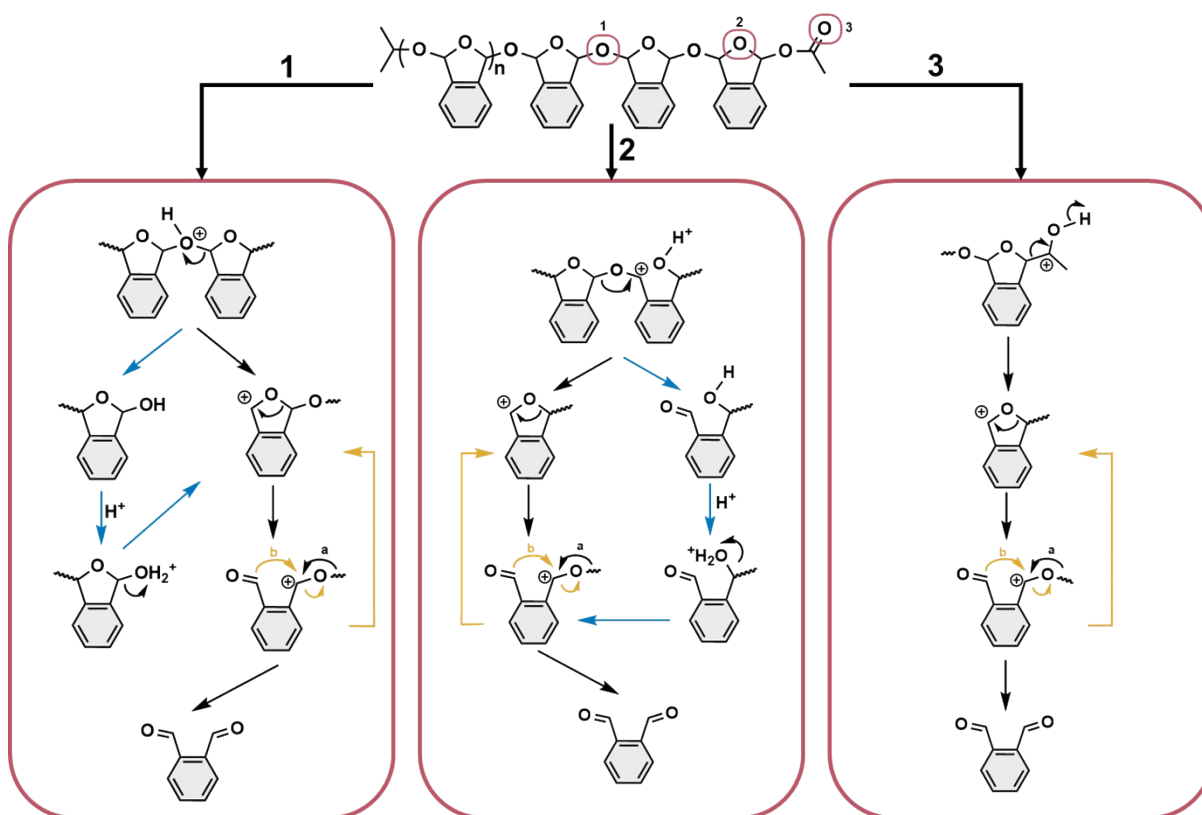


Figure S34. Proposed acid-catalyzed decomposition mechanism of linear PPA.

6. Fluoride-triggered depolymerization of PPA

6.1. Structural stability of PPA in DCM and DMSO solvents

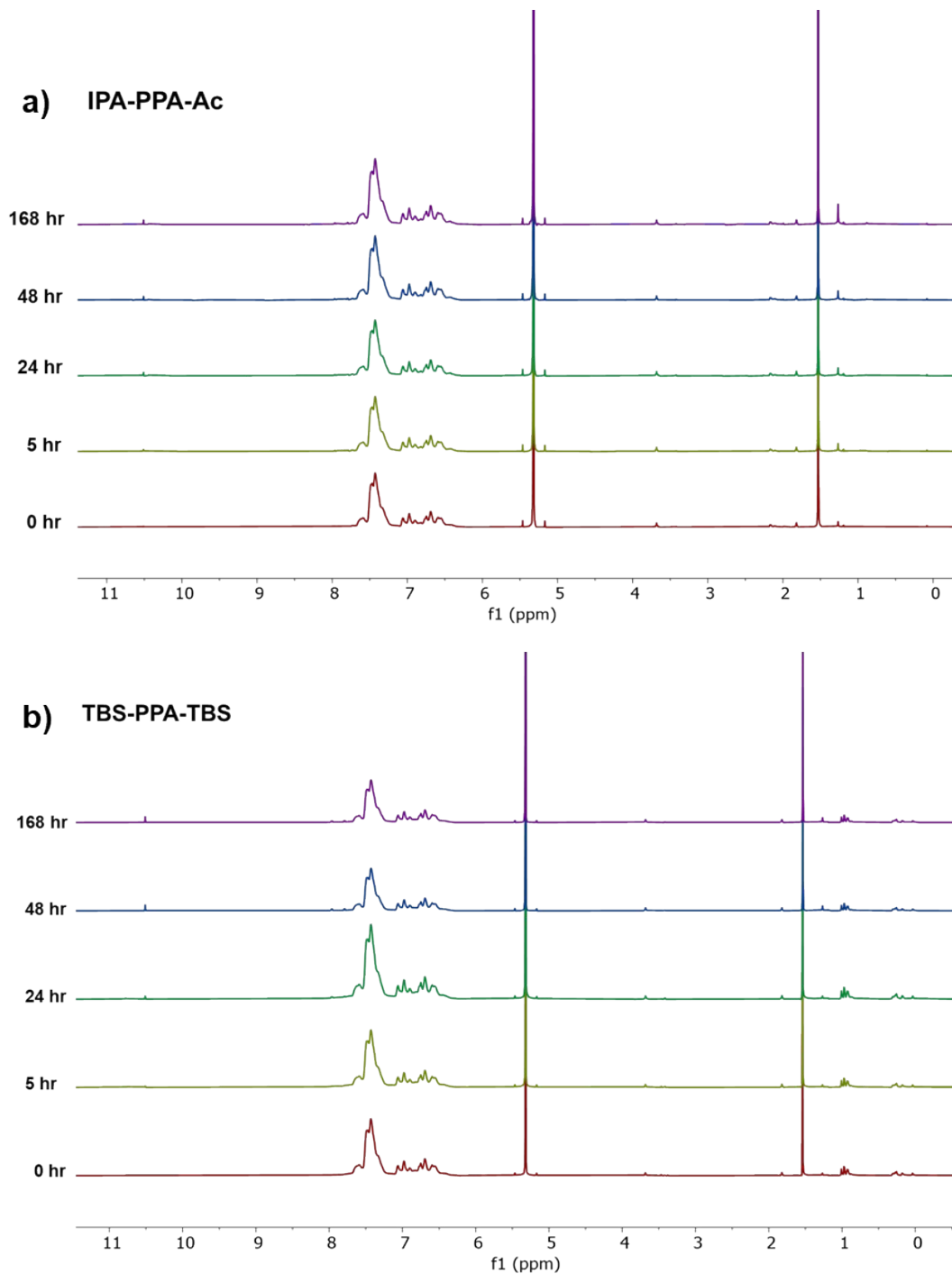


Figure S35. ¹H-NMR spectra of IPA-PPA-Ac and TBS-PPA-TBS in DCM-d₂, suggesting that both polymers are stable for up to 1 week in the solvent.

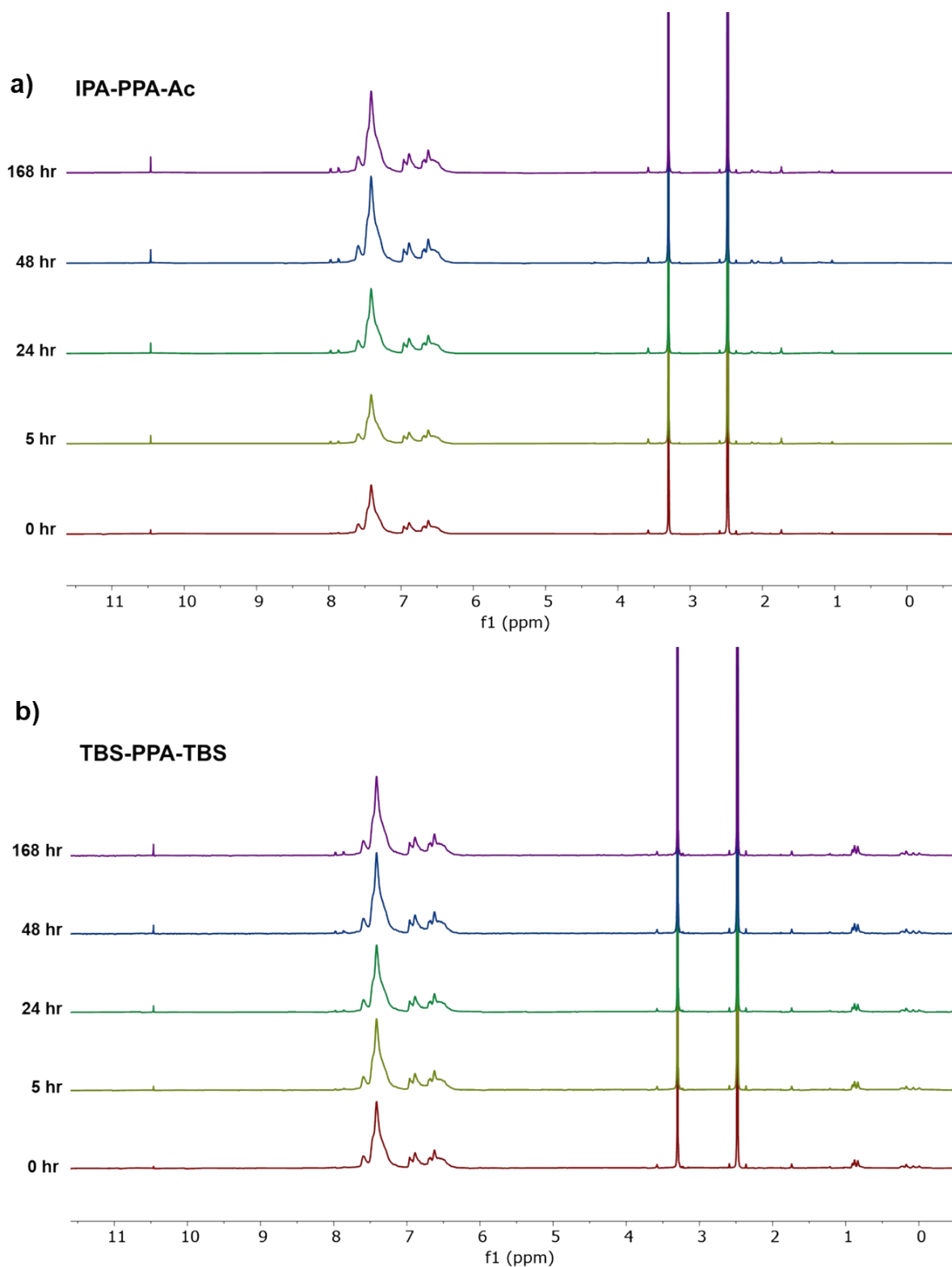


Figure S36. $^1\text{H-NMR}$ spectra of IPA-PPA-Ac and TBS-PPA-TBS in DMSO-d_6 , suggesting that both polymers are stable for up to 1 week in the solvent.

6.2. Fluoride-triggered depolymerization of TBS-PPA-TBS

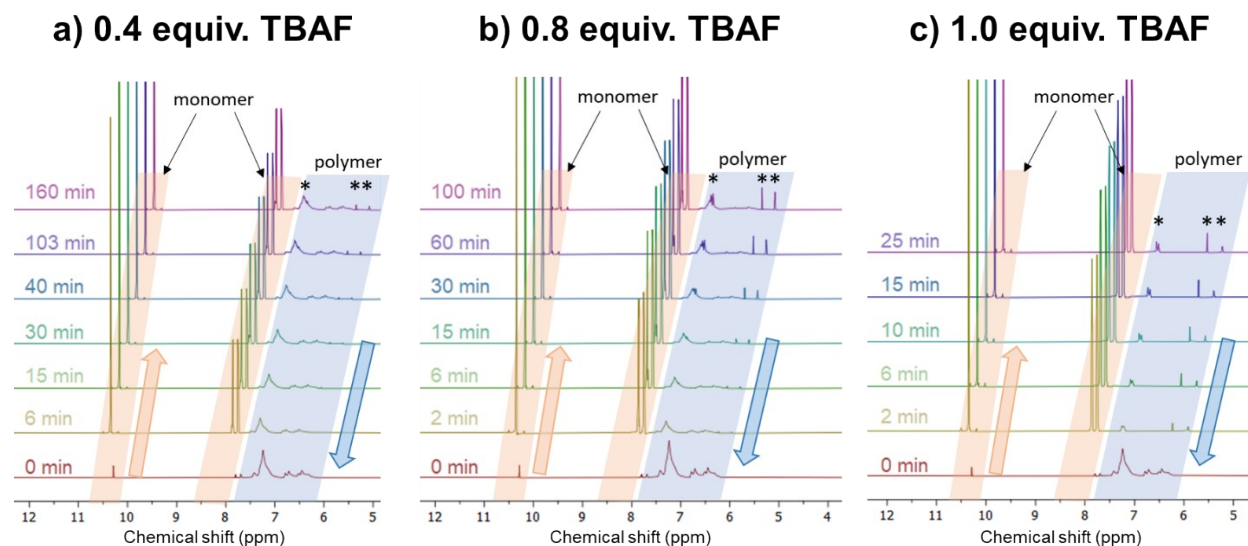


Figure S37. The variation in the $^1\text{H-NMR}$ spectra of TBS-PPA-TBS upon exposure to various doses of TBAF at different time intervals. The asterisk "*" refers to peaks of unidentified by-products.

Polymer	[Polymer]	M.W (KDa)	[F ⁻]	F ⁻ equiv. rel. to the polymer	Solvent	Temp	Time	Ref
poly(benzylether)macro-cross-linker (6)	20 μM	21	50 μM	2.5	THF	23 °C	60 mins	10
poly(benzylether)macro-cross-linker (7)	1 mM	0.59	4 mM	4.0	THF	23 °C	30 mins	10
End-Capped Poly-(benzyl ether)	0.144 μM	165	8.35 μM	58	100:1 THF-phosphate buffer	18 °C	30 mins	11
End-Capped Poly(phthalaldehydes)	1.6 mM	54.2	16 mM	10	63:1 THF-phosphate buffer	23 °C	300 mins	12
fluoride-triggerable polyester (P4)	1 mM	7.7	1 M	1000	20:1 Acetone-phosphate buffer	37 °C	45% in 48 hrs	13
fluoride-triggerable polyester (P5)	1 mM	8.7	1 M	1000	20:1 Acetone-phosphate buffer	37 °C	60% in 48 hrs	13
Polymer thermoset (6)	0.05 M	47	1 M	20	20:1 DMF-THF	RT	40 mins	14
Deep eutectic solvent (DES)-based polymer thermosets	-	-	1 M	-	MeOH	25 °C	180 min	15
Cationic Poly(benzyl ether) (P0-S-4.9)	1 M	4.9	1 M	1.0	THF	RT	16 hrs	16
poly(benzyl ether)s (P ₁ -50-PEG ₈₀₀)	-	3.4	-	3.0	MeOH	RT	16 hrs	17
poly(VBpin-co-MMA)	30 mM	17.5	75 mM	2.5	1,4-Dioxane	RT	38% in 24 hrs	18
TBS-PPA-TBS	0.5 mM	12.9	0.5 mM	1.0	DMSO	RT	2 mins	This work

Table S4. Comparison of depolymerization rate towards fluorides among prevailing self-immolative polymers.

6.3. Integrated rate laws

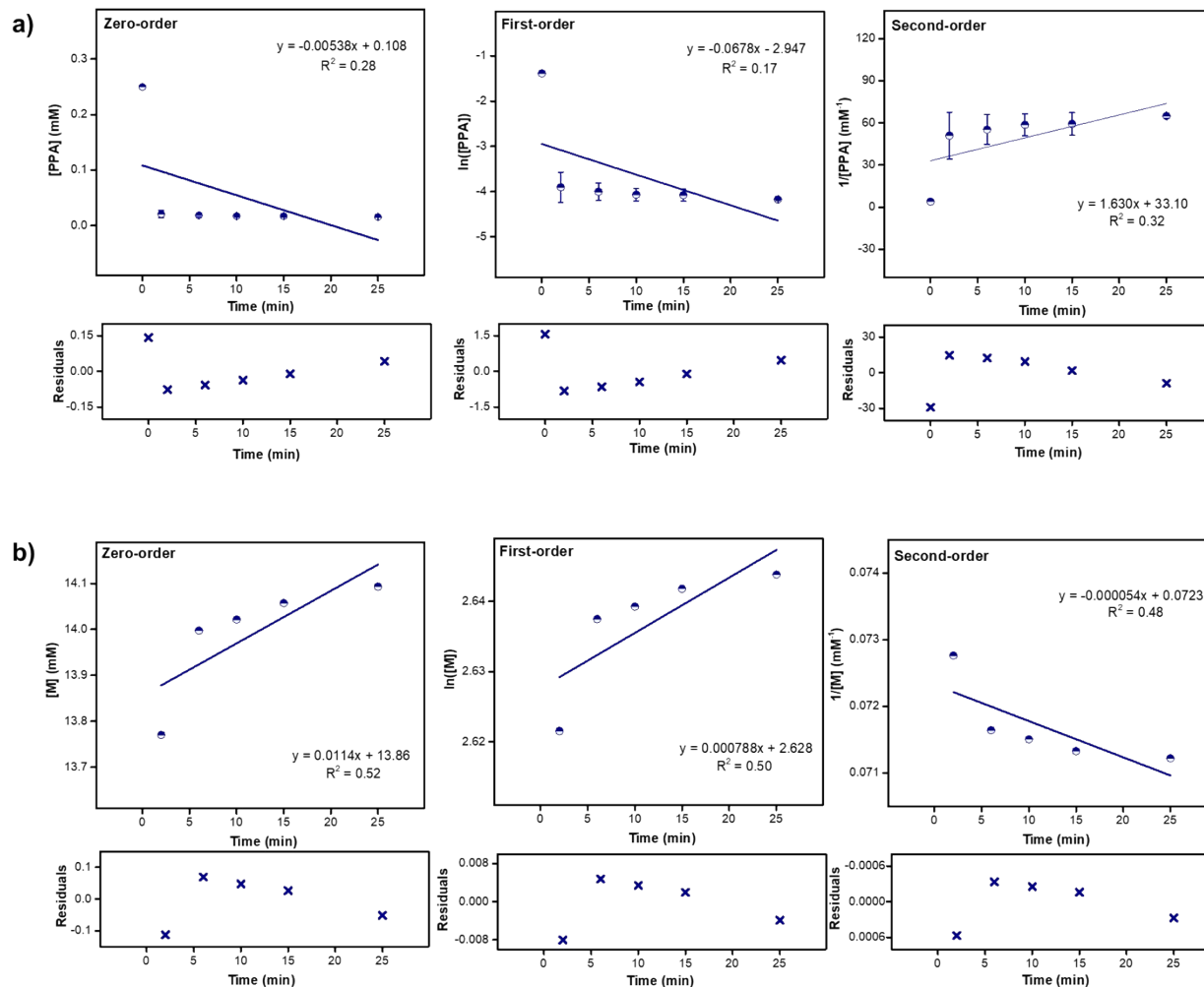


Figure S38. Kinetic study of TBS-PPA-TBS depolymerization according to a) polymer and b) monomer. Zero-order, first-order, and second order plots of the depolymerization at 1.0 equiv. of TBAF.

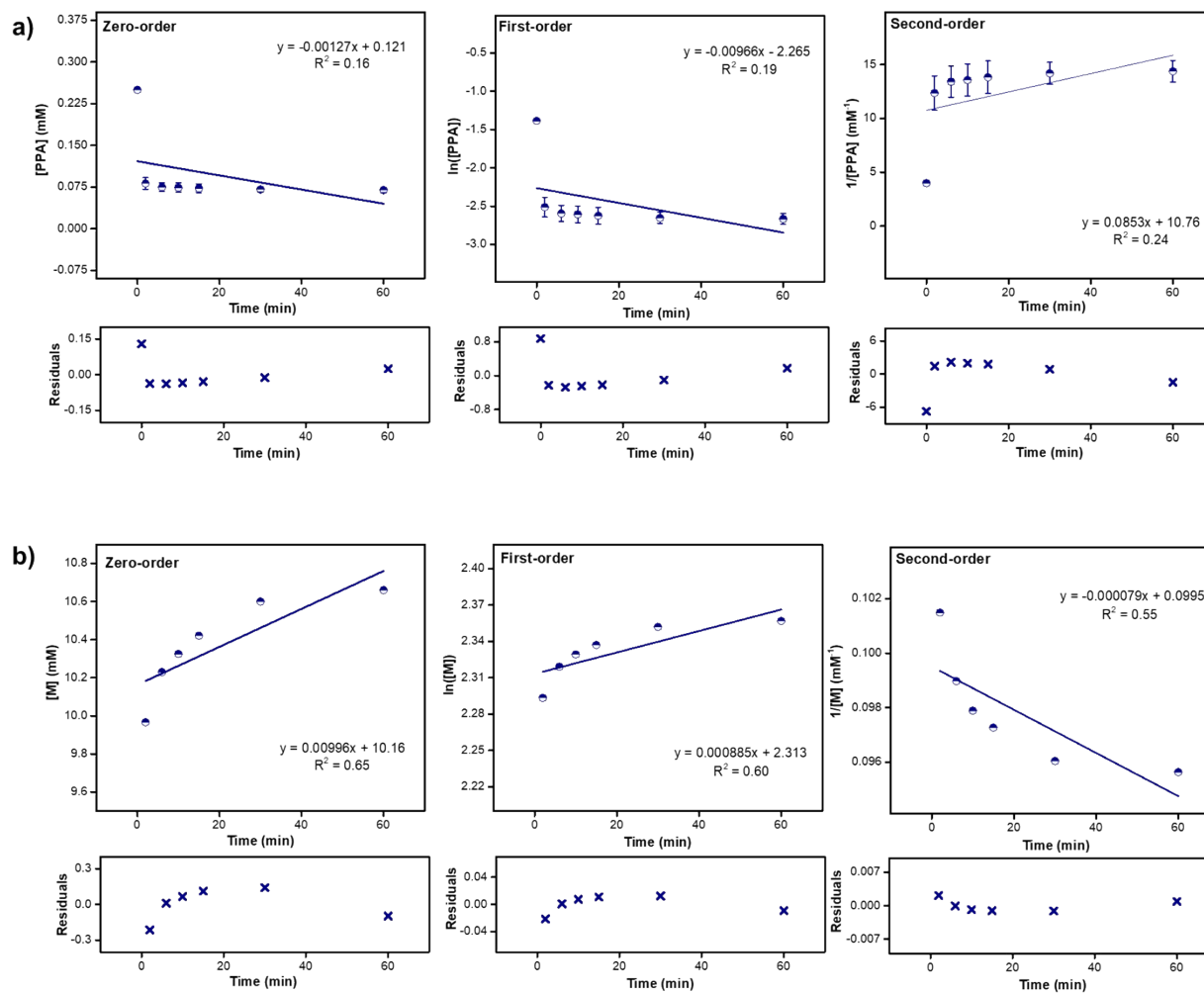


Figure S39. Kinetic study of TBS-PPA-TBS depolymerization according to a) polymer and b) monomer. Zero-order, first-order, and second order plots of the depolymerization at 0.8 equiv. of TBAF.

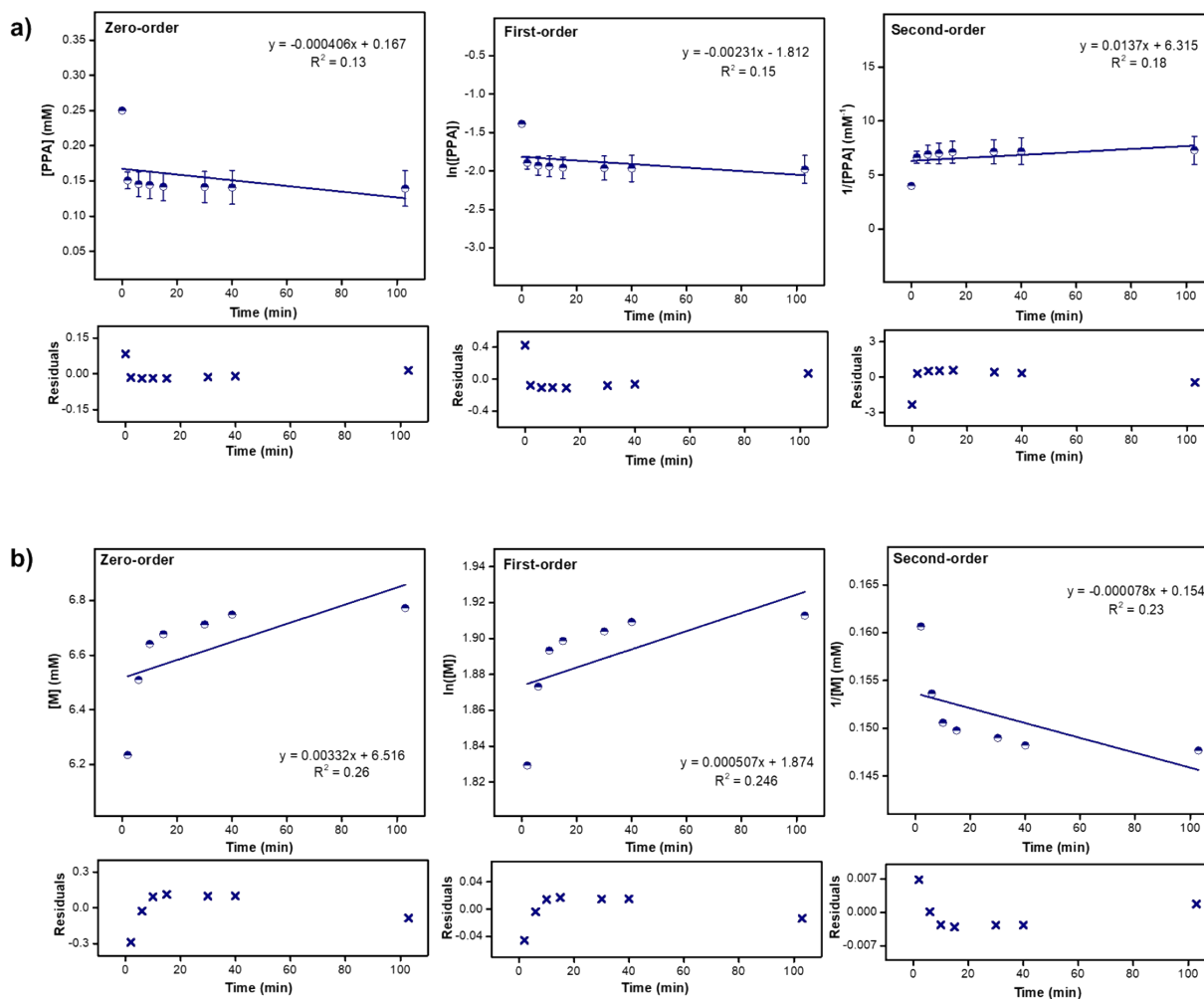


Figure S40. Kinetic study of TBS-PPA-TBS depolymerization according to a) polymer and b) monomer. Zero-order, first-order, and second order plots of the depolymerization at 0.4 equiv. of TBAF.

6.4. Rapid kinetic screening of TBS-PPA-TBS decomposition

Due to the fast degradation rate of TBS-PPA-TBS when exposed to 1.0 eq of TBAF, we reasoned that a finer measurement technique is needed to closely monitor the depolymerization rate, especially in the first 3 minutes of the reaction. Our initial kinetic data showed that a near-complete depolymerization was attained after 2 minutes of exposing TBS-PPA-TBS to fluorides ions.

To clarify why the first data point in the depolymerization kinetics experiments was recorded after 2 minutes of the addition of the stimulus, we need to go over the basic protocol followed for acquiring each NMR spectrum, which involves the following four commands. 1) Atma: stands for automatic tuning and matching. It is used to tune the probe frequency to match the nuclei. 2) Lock: used to keep a homogeneous magnetic field during an experiment by ensuring that the strength of the magnetic field surrounding the sample is not changing. 3) Shim: used to correct any inhomogeneities in the applied magnetic field. 4) RGA: stands for receiver gain automatic and is used to regulate the amplitude of the free induction decay before it is sent to the digitizer. The overall time needed for these commands is approximately 80 seconds, which after being added to the scan time needed to obtain the spectrum, totals up to approximately 2 minutes per sample. To attain a spectrum every 10 seconds following the addition of TBAF, several adjustments were made to the abovementioned protocol. First, we have reduced the number of scans from 16 to 2 scans, which allowed us to collect a spectrum in only 7 seconds of scanning time. We noted no significant change in the initial NMR spectrum for PPA when collected over 2 and 16 scans, which affirmed that we can still get somewhat accurate spectra and hence integrations even with 2 scans. Second, we ran the sample at $t_0 = 0$ sec, which corresponds to TBS-PPA-TBS before the addition of TBAF, following the protocols listed above and collected the spectrum after 2 scans only. We then saved the lock and shim parameters obtained for the initial sample and applied all of them to the consequent measurements after the addition of TBAF. In other words, following the addition of TBAF (1.0 eq relative to PPA), the first and only step was to collect 2 scans for the mixture every 10 seconds. In this way, we were able to monitor the depolymerization rate every 10 seconds for the first 3 minutes.

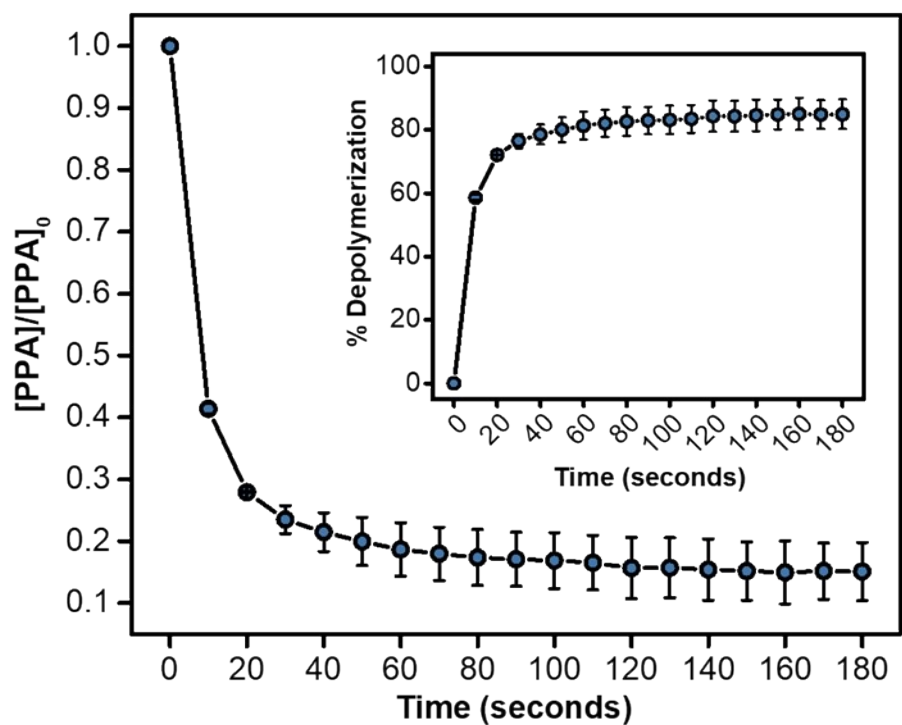


Figure S41. Fluoride-catalyzed degradation kinetics of TBS-PPA-TBS after exposure to 1.0 eq of TBAF for the first 3 minutes of the depolymerization reaction.

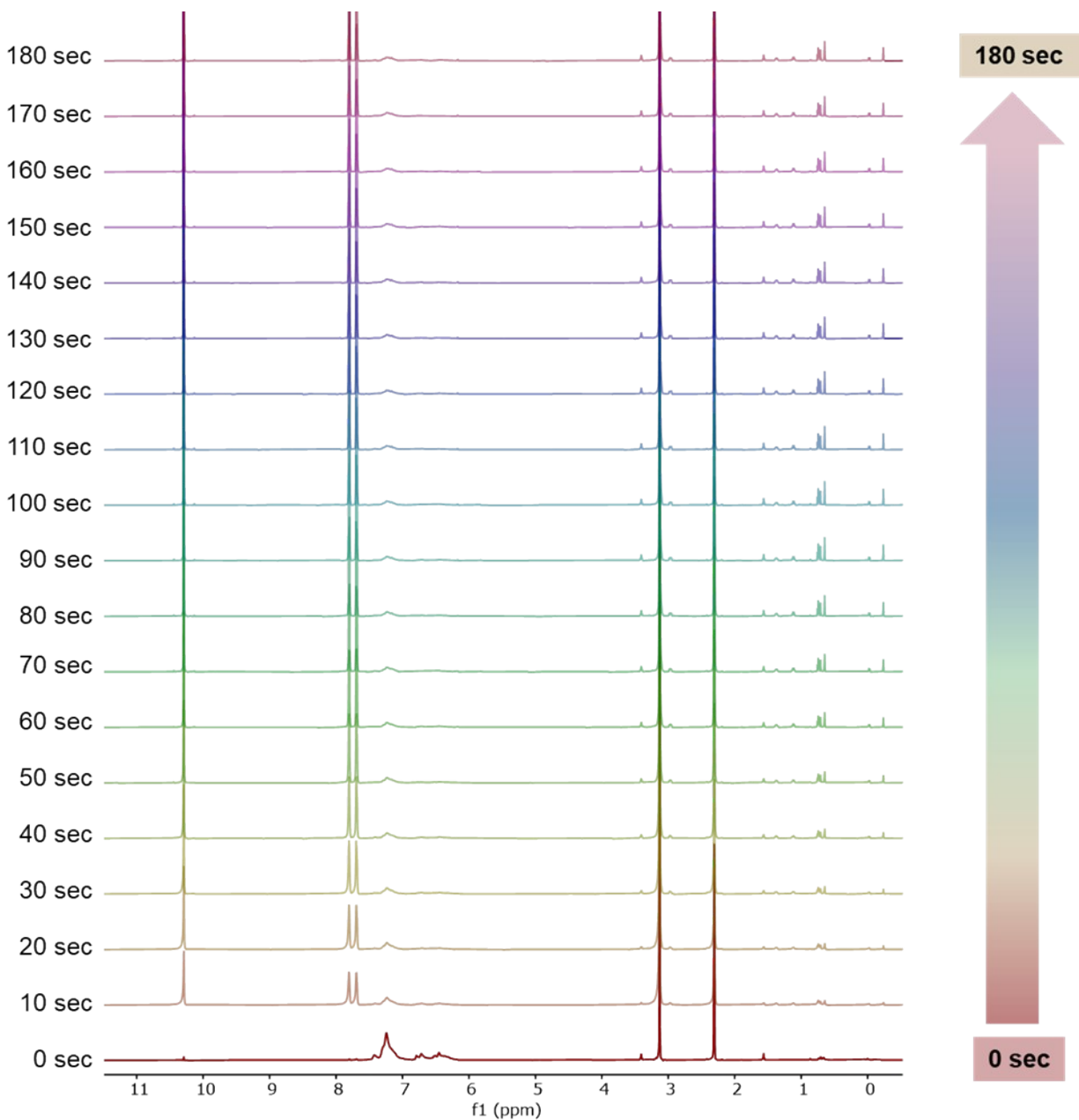


Figure S42. Stacked plot of time-resolved in situ NMR spectra of TBS-PPA-TBS after exposure to 1.0 eq of TBAF showing the rapid degradation of the polymer from the moment TBAF is added. NMR spectra are collected in DMSO- d_6 (2 scans/time interval) and room temperature.

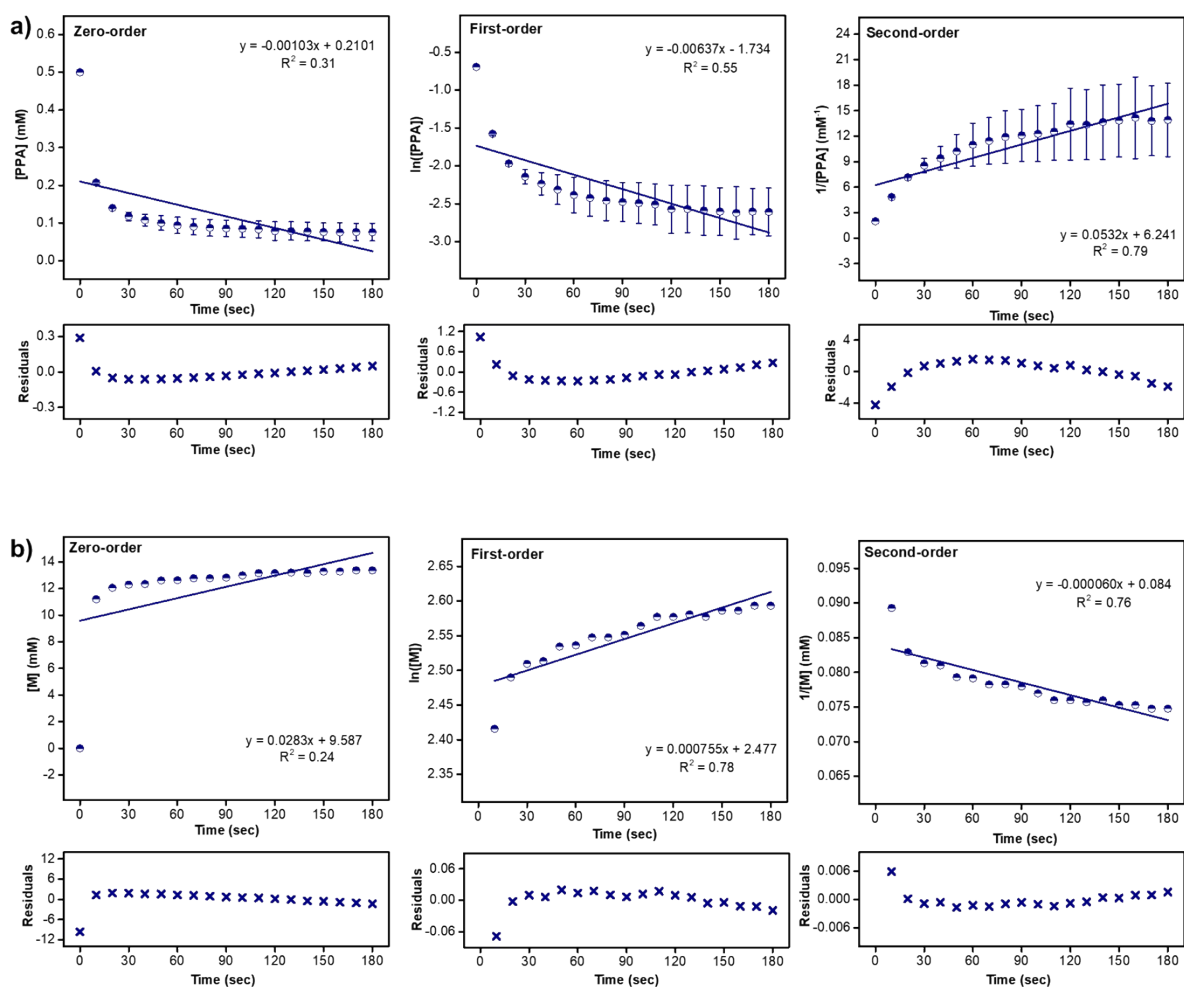


Figure S43. Kinetic study of TBS-PPA-TBS depolymerization according to a) polymer and b) monomer. Zero-order, first-order, and second order plots of the depolymerization at 1.0 equiv. of TBAF for the first 3 minutes of the depolymerization reaction.

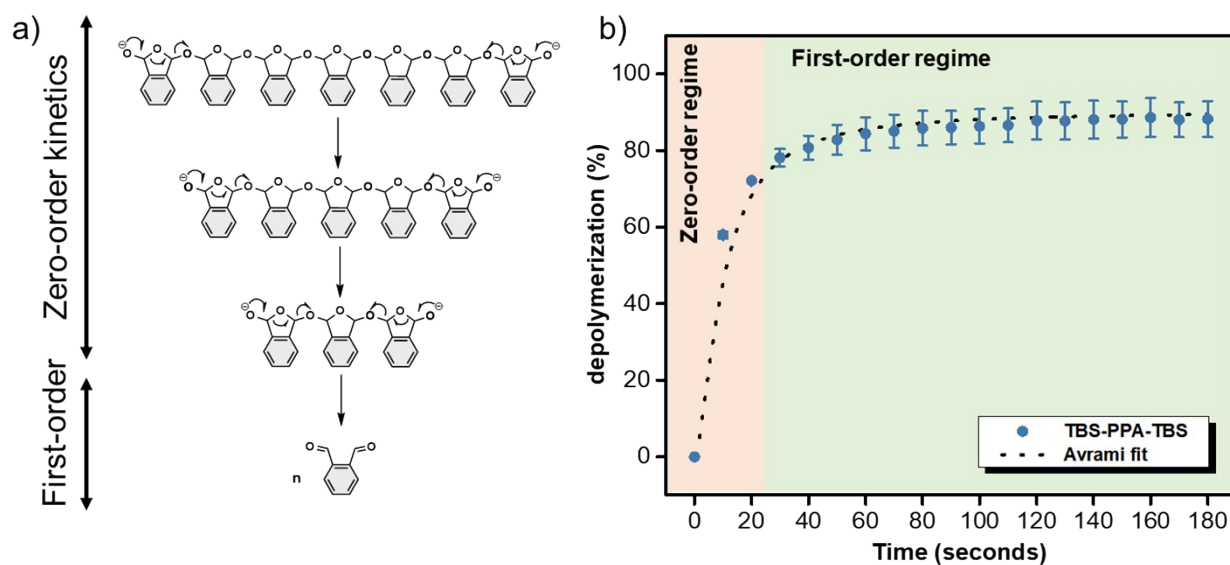


Figure S44. Proposed mixed-mode decomposition profile for the depolymerization of TBS-PPA-TBS in response to fluoride ions involving an initial zero-order regime followed by a gradual transition toward first-order regime.

The polymer degradation data found above were fit to a modified Avrami equation¹⁹ of the form:

$$P_t = e^{-(k.t)^q} \quad \text{Equation S4}$$

Where P_t is the percent of polymer decomposed at a time t , k is the effective 1st order rate constant, and q is the adjustment factor.

6.5. Effect of the nature of the tetra-*n*-butylammonium salt on TBS-PPA-TBS degradation rate

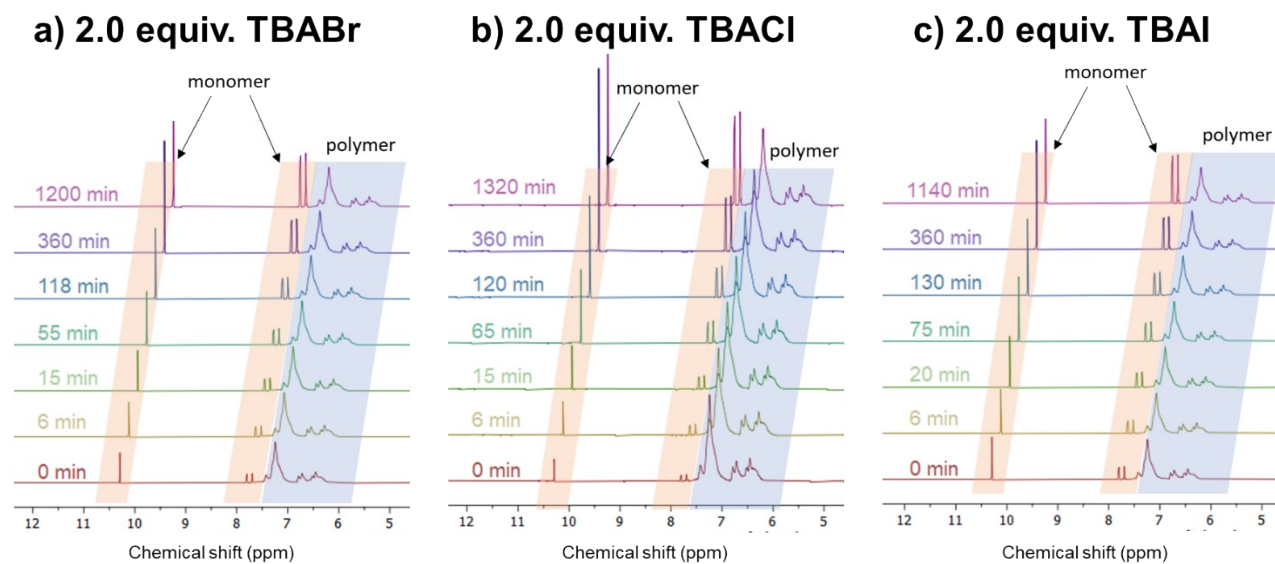


Figure S45. $^1\text{H-NMR}$ spectra of TBS-PPA-TBS after exposure to 2.0 equivalences of tetrabutylammonium halides.

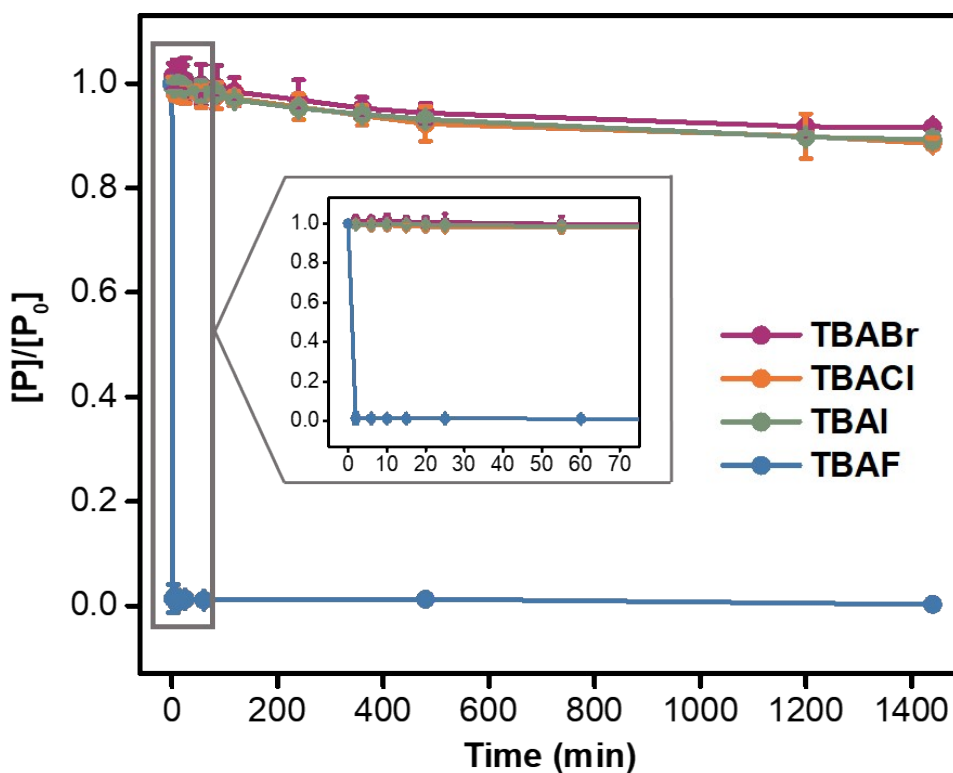


Figure S46. Degradation rate of TBS-PPA-TBS in response to 2.0 equivalences of TBAF, TBABr, TBACl, and TBAI.

6.6. Mechanism of fluoride-catalyzed degradation of TBS-PPA-TBS

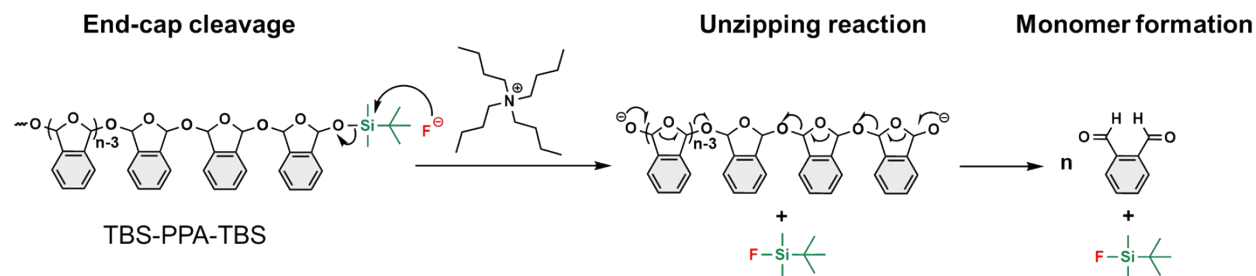


Figure S47. Potential degradation mechanism of TBS-PPA-TBS in response to fluoride-mediated endcap cleavage.

7. Solid-state depolymerization (SSD)

7.1 Preparation of TBS-PPA-TBS disks

In a 4 mL scintillation vial, 100 mg of TBS-PPA-TBS ($M_n \sim 12.9$ kDa) were dissolved in 0.5 mL of dry dichloromethane. The solution was then vortexed for a few seconds to allow the complete dissolution of the polymer. Using a 1 mL syringe, the solution was drop-casted into a silicon mold and left on the bench for 48 hours to allow complete evaporation of the solvent.

7.2 Solid-state depolymerization (SSD) of TBS-PPA-TBS

For the solid-state depolymerization experiment, we used solvents that can neither depolymerize nor dissolve PPA. We found acetone the best solvent to suspend PPA in due to its low solubility and poor solubilizing capacity towards PPA. In addition, ethyl acetate was chosen to dissolve TBAF due to its inability to solvate the polymer. In brief, after leaving a 7 mg PPA disk suspended in 1.5 mL acetone for a few hours to ensure no depolymerization occurred, 2 mM of an F^- solution (1 drop) in ethyl acetate was added to the PPA solution and the polymer was left to decompose at room temperature without stirring. Within 140 seconds, the polymer solution turned from colorless to pale yellow (which is the original color of the monomer), affirming the capacity of PPA to depolymerize in the solid-state when in contact with a minimal concentration and volume of fluoride trigger.

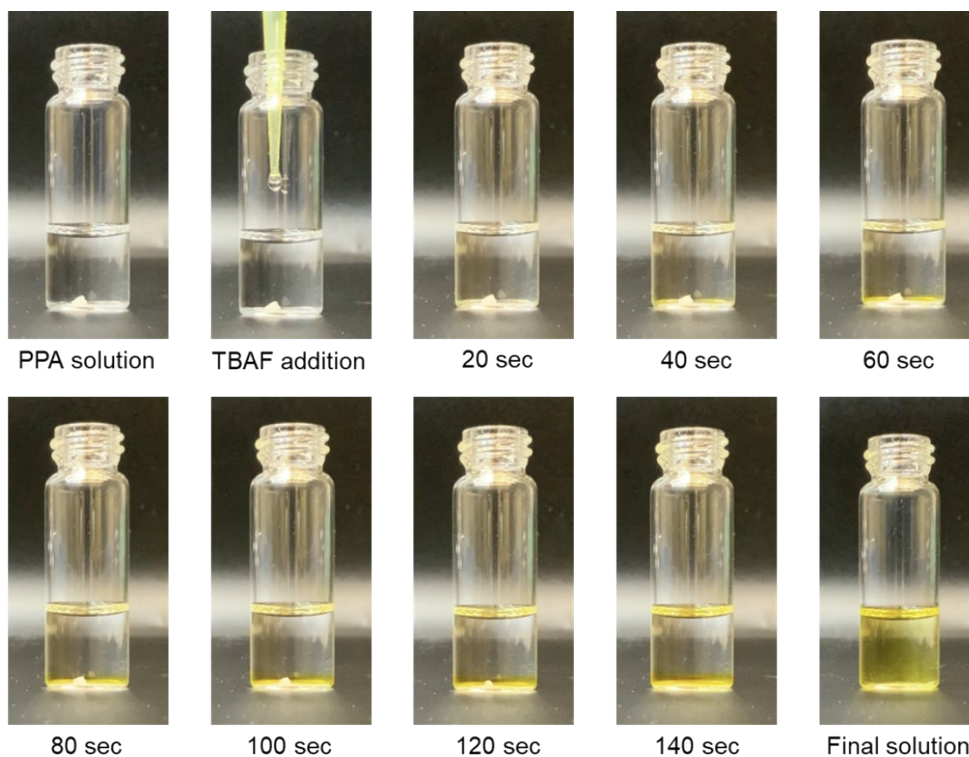


Figure S48. Solid-state depolymerization of TBS-PPA-TBS upon exposure to 2.0 mM of TBAF.

7.3 Characterization of the SSD experiment product.

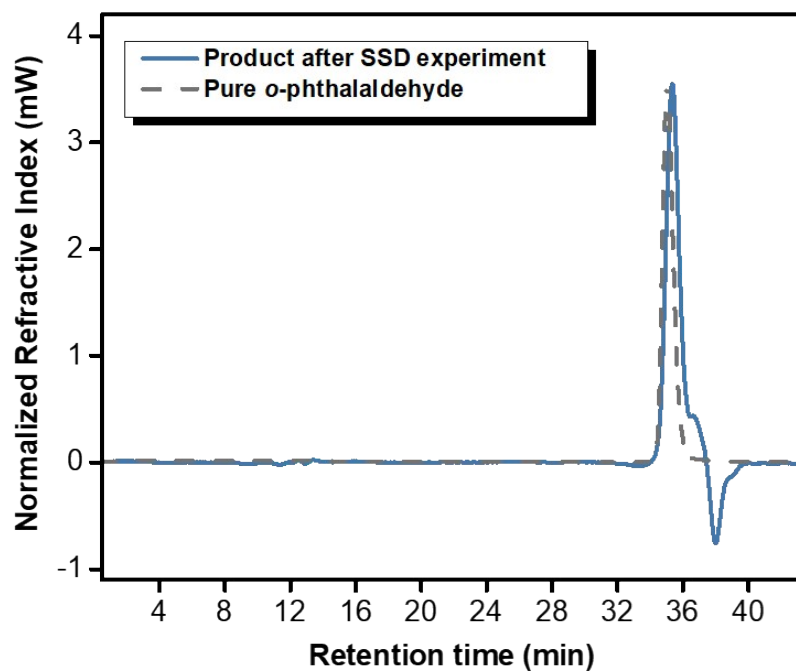


Figure S49. Representative GPC elution curves of pure *o*-phthalaldehyde and the product obtained after the solid-state depolymerization experiment.

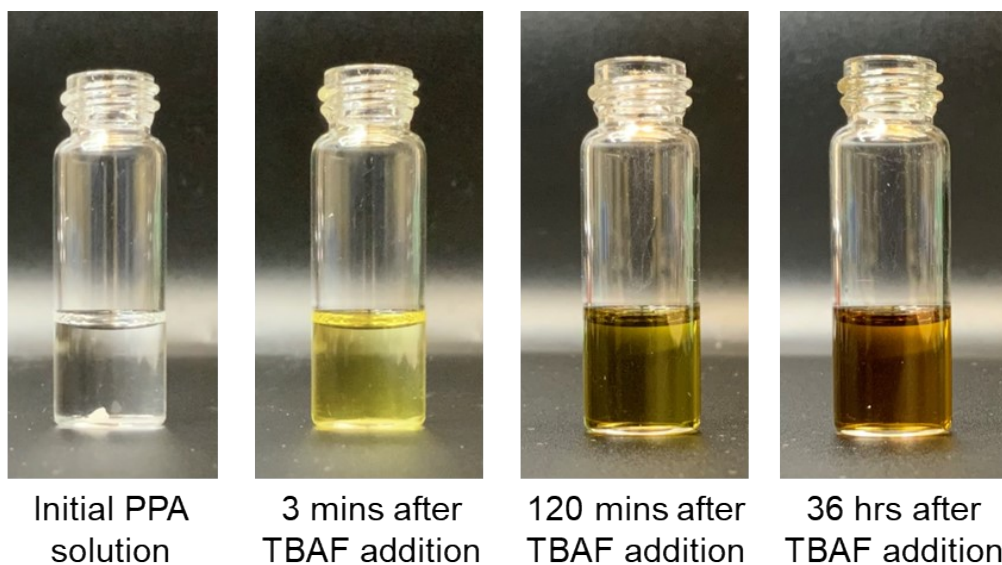


Figure S50. Solid-state depolymerization of TBS-PPA-TBS by TBAF after different periods of time at room temperature.

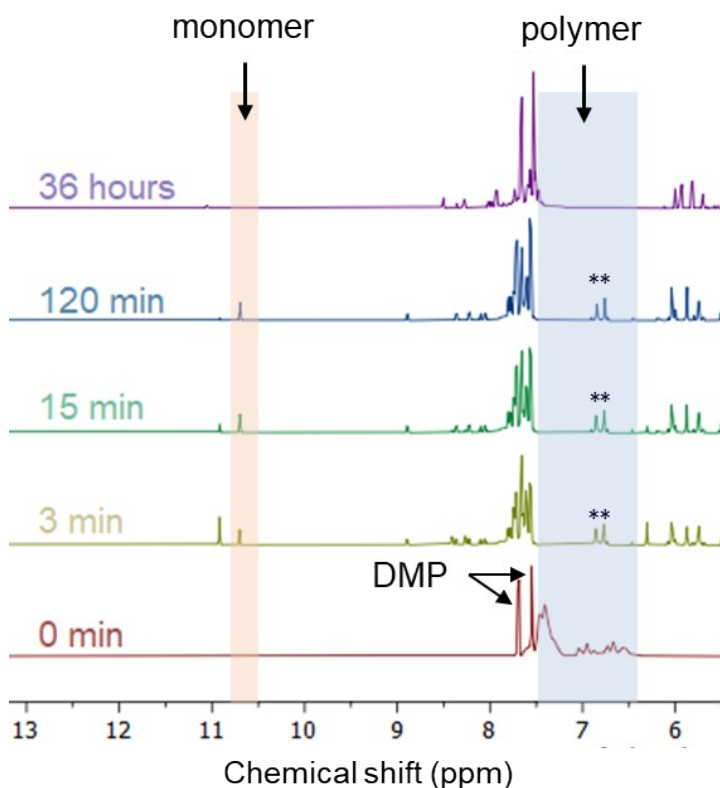


Figure S51. $^1\text{H-NMR}$ spectra of the solid-state depolymerization experiment of TBS-PPA-TBS by TBAF after different periods of time at room temperature. The asterisk “*” refers to unidentified side products.

8. Preparation of NYCO-bonded textiles on glass substrates

NYCO wrapped textiles with linear PPA were prepared via a melt bonding method. In brief, 100 mg of PPA were dissolved in 0.55 mL of dichloromethane followed by sonication for a few seconds to ensure a complete dissolution of the polymer. This was followed by the addition of 20% w/w of DMP relative to PPA, which corresponds to 16.8 μ L to the solution, and the resulting mixture was vortexed for a few seconds and left on the bench. In the meantime, the NYCO wrapped slides were prepared by wrapping a glass slide with strips of NYCO swatch and gluing the ends of the textile on the back edge of the slide as seen in **Figure S51**.

Bonding NYCO textiles using the solvent bonding, or the melt bonding methods proved to be challenging as the PPA solution was penetrating and diffusing through the fabric and hence very little amount of PPA was sticking to the surface of the textile. For this reason, we opted to bind textiles with PPA films rather than with liquid phase PPA. In short, the PPA/DMP solution prepared was drop casted using a syringe into a silicone mold and left on the bench for 48 hours to ensure complete evaporation of the DCM solvent. The resulting PPA film was transferred onto the surface of a NYCO wrapped slide. Subsequently, the minimal amount of DCM needed to dissolve the film was added dropwise (<0.1 mL) and the textile slide was immediately heated for a few seconds on a hot plate at 80°C to remove excess solvent. The second NYCO wrapped slide was later placed on top such that the overlap area of the substrates was approximately 20% the length of the bottom slide initially containing the polymeric mixture.

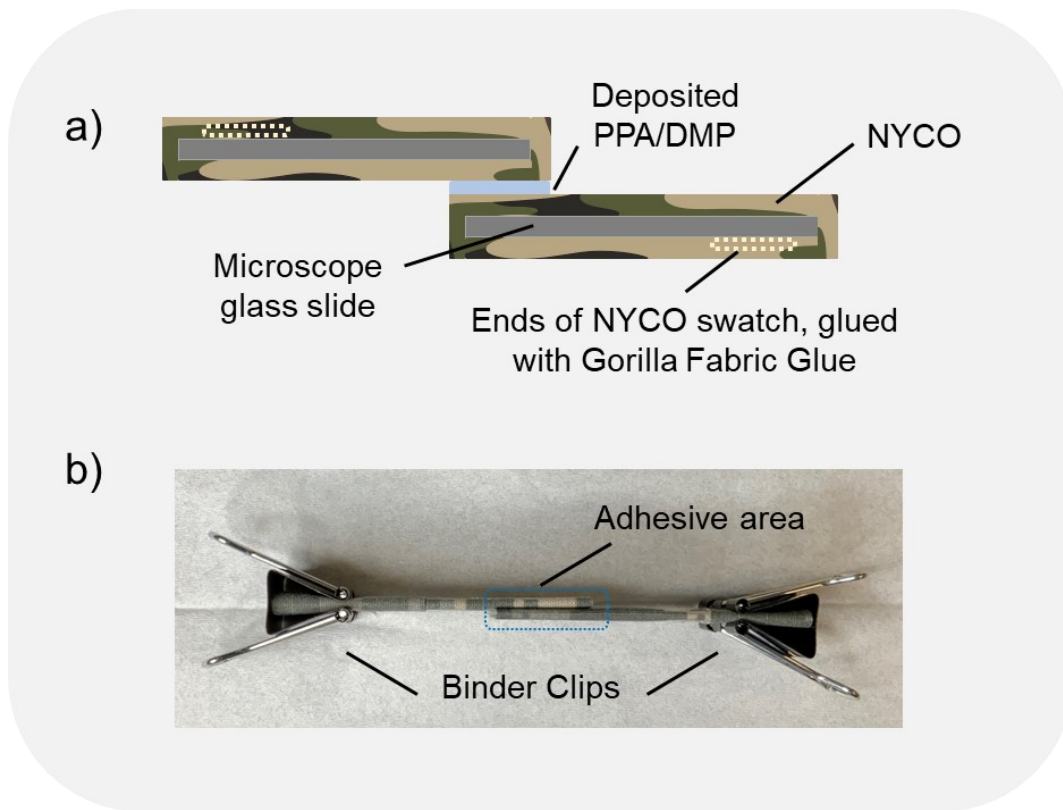


Figure S52. a) Schematic illustration and b) photograph profile of NYCO wrapped slides with linear PPA.

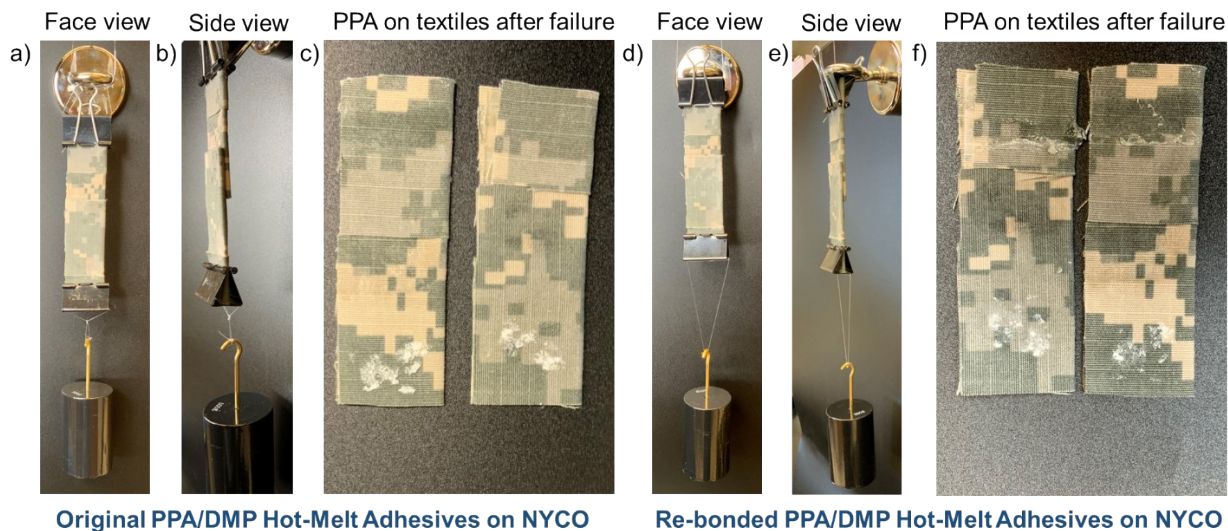


Figure S53. Snapshots showing NYCO-bonded slides with PPA polymer loading a 0.5 kg weight (Original and after rebonding). a) face view, b) side view, c) resulting slides with residuals PPA after debonding using a 1.5 kg weight, d) face view, e) side view, and f) resulting slides with residuals PPA after first mechanical failure using a 1.5 kg weight.

9. References

1. Law, M.; Jackson, D., Residual plots for linear regression models with censored outcome data: A refined method for visualizing residual uncertainty. *Commun. Stat. Simul.* **2017**, *46* (4), 3159-3171.
2. Altman, N.; Krzywinski, M., Regression diagnostics. *Nat. Methods.* **2016**, *13* (5), 385-386.
3. Kaitz, J. A.; Diesendruck, C. E.; Moore, J. S., End Group Characterization of Poly(phthalaldehyde): Surprising Discovery of a Reversible, Cationic Macrocyclization Mechanism. *J. Am. Chem. Soc.* **2013**, *135* (34), 12755-12761.
4. Schwartz, J. M.; Phillips, O.; Engler, A.; Sutlief, A.; Lee, J.; Kohl, P. A., Stable, High-Molecular-Weight Poly(phthalaldehyde). *J. Polym. Sci., Part A: Polym. Chem.* **2017**, *55* (7), 1166-1172.
5. Peterson, G. I.; Boydston, A. J., Kinetic Analysis of Mechanochemical Chain Scission of Linear Poly(phthalaldehyde). *Macromol. Rapid Commun.* **2014**, *35* (18), 1611-1614.
6. DiLauro, A. M.; Phillips, S. T., End-capped poly(4,5-dichlorophthalaldehyde): a stable self-immolative poly(aldehyde) for translating specific inputs into amplified outputs, both in solution and the solid state. *Polym. Chem.* **2015**, *6* (17), 3252-3258.
7. da Costa, V. C.; dos Santos, E. R. F.; de Souza Jr, F. G., Poly(Butylene Succinate) Molar Mass Calculation by GPC and ¹H-NMR. *Macromol. Symp.* **2021**, *398* (1), 2000216.
8. Liu, J.; Loewe, R. S.; McCullough, R. D., Employing MALDI-MS on Poly(alkylthiophenes): Analysis of Molecular Weights, Molecular Weight Distributions, End-Group Structures, and End-Group Modifications. *Macromolecules* **1999**, *32* (18), 5777-5785.
9. Tian, Y.; Kuzimenkova, M. V.; Halle, J.; Wojdyr, M.; Diaz de Zerio Mendaza, A.; Larsson, P.-O.; Müller, C.; Scheblykin, I. G., Molecular Weight Determination by Counting Molecules. *J. Phys. Chem. Lett.* **2015**, *6* (6), 923-927.
10. Kim, H.; Mohapatra, H.; Phillips, S. T., Rapid, On-Command Debonding of Stimuli-Responsive Cross-Linked Adhesives by Continuous, Sequential Quinone Methide Elimination Reactions. *Angew. Chem. Int. Ed.* **2015**, *54* (44), 13063-13067.
11. Olah, M. G.; Robbins, J. S.; Baker, M. S.; Phillips, S. T., End-Capped Poly(benzyl ethers): Acid and Base Stable Polymers That Depolymerize Rapidly from Head-to-Tail in Response to Specific Applied Signals. *Macromolecules* **2013**, *46* (15), 5924-5928.
12. DiLauro, A. M.; Abbaspourrad, A.; Weitz, D. A.; Phillips, S. T., Stimuli-Responsive Core-Shell Microcapsules with Tunable Rates of Release by Using a Depolymerizable Poly(phthalaldehyde) Membrane. *Macromolecules* **2013**, *46* (9), 3309-3313.
13. Kan, X.-W.; Zhang, L.-J.; Li, Z.-Y.; Du, F.-S.; Li, Z.-C., Fluoride-Triggered Self-Degradation of Poly(2,4-disubstituted 4-hydroxybutyric acid) Derivatives. *Macromol. Rapid Commun.* **2021**, *42* (18), 2100169.
14. Oh, Y.; Park, J.; Park, J.-J.; Jeong, S.; Kim, H., Dual Cross-Linked, Polymer Thermosets: Modular Design, Reversible Transformation, and Triggered Debonding. *Chem. Mater.* **2020**, *32* (15), 6384-6391.
15. Jung, S. H.; Choi, G.; Jeong, S.; Park, J.; Yoon, H.; Park, J.-J.; Kim, H., Synthesis of Stimuli-Responsive, Deep Eutectic Solvent-Based Polymer Thermosets for Debondable Adhesives. *ACS Sustain. Chem. Eng.* **2022**, *10* (41), 13816-13824.
16. Ergene, C.; Palermo, E. F., Cationic Poly(benzyl ether)s as Self-Immolative Antimicrobial Polymers. *Biomacromolecules* **2017**, *18* (10), 3400-3409.
17. Ergene, C.; Palermo, E. F., Self-immolative polymers with potent and selective antibacterial activity by hydrophilic side chain grafting. *J. Mater. Chem. B.* **2018**, *6* (44), 7217-7229.
18. Makino, H.; Nishikawa, T.; Ouchi, M., Polymer Degradation by Synergistic Dual Stimuli: Base Interaction and Photocatalysis to Unlock a Boron Pendant Trigger for Main-Chain Scission. *Macromolecules* **2023**.

19. Bystritskaya, E. V.; Karpukhin, O. N.; Kutsenova, A. V., Monte Carlo Simulation of Linear Polymer Thermal Depolymerization under Isothermal and Dynamic Modes. *Int. J. Polym. Sci.* **2011**, *2011*, 849370.